EMBO Molecular Medicine

Inhibition of transglutaminase 2 mitigates transcriptional dysregulation in models of Huntington's disease

Stephen J. McConoughey[1,2,14†], Manuela Basso[1,2,†], Zoya V. Niatsetskaya[1,2], Sama F. Sleiman[1,2], Natalia A. Smirnova[1,2], Brett C. Langley[1,2], Lata Mahishi[1,2], Arthur J. L. Cooper[3], Marc A. Antonyak[4], Rick A. Cerione[4], Bo Li[4], Anatoly Starkov[2], Rajnish Kumar Chaturvedi[2,15], M. Flint Beal[2], Giovanni Coppola[5], Daniel H. Geschwind[5], Hoon Ryu[6], Xia Li[1], Siiri E. Lismaa[7], Judit Pallos[8], Ralf Pasternack[9], Martin Hils[9], Jing Fan[10,12], Lynn A. Raymond[12,11], J. Lawrence Marsh[8], Leslie M. Thompson[13], Rajiv R. Ratan[1,2*]*

Keywords: transglutaminase, Huntington's disease, transcriptional dysregulation, mitochondrial bioenergetics, ZDON

DOI 10.1002/emmm.201000084

Received August 04, 2009
Revised June 18, 2010
Accepted June 23, 2010

→See accompanying Closeup by Kazemi-Esfarjani and La Spada: http://dx.doi.org/10.1002/emmm.201000092

Caused by a polyglutamine expansion in the huntingtin protein, Huntington's disease leads to striatal degeneration via the transcriptional dysregulation of a number of genes, including those involved in mitochondrial biogenesis. Here we show that transglutaminase 2, which is upregulated in HD, exacerbates transcriptional dysregulation by acting as a selective corepressor of nuclear genes; transglutaminase 2 interacts directly with histone H3 in the nucleus. In a cellular model of HD, transglutaminase inhibition de-repressed two established regulators of mitochondrial function, PGC-1α and cytochrome *c* and reversed susceptibility of human HD cells to the mitochondrial toxin, 3-nitroproprionic acid; however, protection mediated by transglutaminase inhibition was not associated with improved mitochondrial bioenergetics. A gene microarray analysis indicated that transglutaminase inhibition normalized expression of not only mitochondrial genes but also 40% of genes that are dysregulated in HD striatal neurons, including chaperone and histone genes. Moreover, transglutaminase inhibition attenuated degeneration in a *Drosophila* model of HD and protected mouse HD striatal neurons from excitotoxicity. Altogether these findings demonstrate that selective TG inhibition broadly corrects transcriptional dysregulation in HD and defines a novel HDAC-independent epigenetic strategy for treating neurodegeneration.

(1) Burke Medical Research Institute, White Plains, NY, USA.
(2) Department of Neurology and Neuroscience, Weill Medical College of Cornell University, New York, NY, USA.
(3) Department of Biochemistry and Molecular Biology, New York Medical College, Valhalla, NY, USA.
(4) Department of Molecular Medicine, Cornell University, Ithaca, NY, USA.
(5) Program in Neurogenetics, Department of Neurology, David Geffen School of Medicine, University of California at Los Angeles, Los Angeles, CA, USA.
(6) Department of Neurology, Boston University School of Medicine, Boston, MA, USA.
(7) Victor Chang Cardiac Research Institute, University of New South Wales, Darlinghurst, NSW, Australia.
(8) Department of Developmental and Cell Biology, University of California, Irvine, CA, USA.
(9) Zedira GmbH, Darmstadt, Germany.
(10) Graduate Program in Neuroscience, University of British Columbia, Vancouver, British Columbia, Canada.
(11) Department of Psychiatry, University of British Columbia, Vancouver, British Columbia, Canada.
(12) Brain Research Centre, University of British Columbia, Vancouver, British Columbia, Canada.
(13) Departments of Psychiatry and Human Behavior, Neurobiology and Behavior and Biological Chemistry, University of California, Irvine, CA, USA.
(14) Current address: Center for Molecular Neurobiology, The Ohio State University, Columbus, OH 43210, USA.
(15) Current address: Developmental Toxicology Division, Indian Institute of Toxicology Research, Lucknow, India.
***Corresponding author:** Tel: +1-914-597-2851; Fax: +1-914-597-2225
E-mail: mbasso@burke.org; rrr2001@med.cornell.edu
†Both authors contributed equally to this work.

INTRODUCTION

Huntington disease (HD) is caused by the expansion of an unstable CAG repeat in the gene encoding the huntingtin (htt) protein. This expanded CAG repeat results in a mutant huntingtin (mhtt) that contains an extended polyglutamine (polyQ) region within its N-terminal region. Although htt is ubiquitously expressed, HD neuropathology centres on the dysfunction and eventual loss of striatal and cortical neurons, particularly of the GABA-ergic medium spiny neurons within the striatum (Vonsattel & DiFiglia, 1998). In the 15 years since the identification of the dynamic mutation responsible for HD, the discoveries of numerous interacting factors, myriad genes that are transcriptionally dysregulated, and the deepening appreciation of aspects of the phenotype that extend beyond the striatum (such as psychosis, diabetes and weight loss), the pathogenesis of the disease seems to be getting only more complex (Petersen & Bjorkqvist, 2006).

Transcriptional dysregulation (with a bias toward the downregulation of target genes) was discovered early in the characterization of mhtt effects (Zuccato & Cattaneo, 2009). The activities of transcription factors and other transcriptional proteins might be altered by abnormal interactions with mhtt or by being sequestered into mhtt-containing inclusions (Benn et al, 2008; Dunah et al, 2002; Steffan et al, 2000; van Roon-Mom et al, 2002). The diabetes and weight loss that afflict patients were early clues to metabolic disruption in HD, and indeed defects in the oxidative phosphorylation pathway and a diminished concentration of ATP are observed within regions of the human brain (Brennan et al, 1985; Browne et al, 1997; Jenkins et al, 1993; Seong et al, 2005; Tabrizi et al, 1999). Additional evidence for the important role of metabolic stress plays in HD is the ability of the metabolic toxin 3-nitroproprionic acid (3-NP, a succinate dehydrogenase (SDH) inhibitor) to mimic several features of the disease (Beal et al, 1993), and the fact that disruption of c-AMP response element binding (CREB)-transcription within the mitochondria augments the toxicity of 3-NP in neuronal cultures (Lee et al, 2005). More recently, it was reported that expression of several nuclear-encoded mitochondrial proteins (cytochrome *c* and cytochrome *c* oxidase (COXIV)) and their coactivator (peroxisome proliferator-activated receptor-gamma coactivator 1 alpha, PGC-1α) is inhibited in multiple HD models as well as post-mortem tissue from the central nervous system (CNS) of HD patients (Cui et al, 2006). A coactivator is a protein or protein complex that increases the likelihood that a gene will be transcribed without interacting directly with the DNA in a sequence specific manner. In this context, PGC-1α regulates not only mitochondrial biogenesis, but also fatty acid oxidation, triglyceride metabolism and gluconeogenesis (Spiegelman, 2007).

Given this evidence for repressed metabolic gene expression, several groups have asked whether transcriptional dysregulation in HD, rather than later-onset metabolic stressors, might underlie the energy deficit observed in mhtt cells. Several lines of evidence led us to focus on one particular candidate transcriptional corepressor: transglutaminase 2 (TG2). First, the transcription factors that control the majority of the nuclear-encoded mitochondrial proteins (specific protein 1 (Sp1), nuclear respiratory factor 1 (NRF-1) and CREB) contain glutamine-rich activation domains, and TG2 modifies glutamine residues in proteins to alter protein–protein interactions (Tatsukawa et al, 2009). These modifications are carried out by TG2 catalysing the inter- or intramolecular cross-linking of a glutamine residue to a lysine residue, or the nucleophilic attack on the carboxamide of a glutamine residue by amines (especially polyamines) (Folk and Finlayson, 1977; Lorand & Conrad, 1984). The transamidating activity of TG2 is induced by micromolar Ca^{2+}, which is increased in HD, and is inhibited by GTP. Second, elevated TG2 activity is observed in HD patients and in various model systems (Karpuj et al, 1999; Lesort et al, 2000), and levels of biomarkers for proteins modified by TG2 are increased in the cerebral spinal fluid of HD patients (γ-glutamyl amines such as γ-glutamyl ε-lysine and several γ-glutamyl polyamines) (Jeitner et al, 2008). Third, homozygous germline deletion of TG2 extends the lifespan of a mouse model of HD (Mastroberardino et al, 2002), although the magnitude of this effect is likely mitigated by compensatory upregulation of other TG isoforms (Mastroberardino, personal communication). We hypothesized that endogenous TG2 can modify activation domains present in transcription factors, reducing their ability to induce transcription of nuclear-encoded metabolic genes; alternatively TG2 might polyaminate N-terminal tails of histone proteins leading to increased electrostatic interaction between positively charged polyamines and negatively charged DNA, thus participating in facultative heterochromatin formation. In either of these models, TG2 hyperactivity, as occurs in HD, would repress an established adaptive transcriptional pathway and thereby render vulnerable striatal neurons incapable of responding to metabolic stress.

A first prediction of both models is that TG2 must be in the nucleus to mediate heretofore unrecognized effects on transcriptional silencing; a second prediction is that selective inhibition of TG2 should normalize transcription in HD models, and that this should be highly correlated with the protective effect of TG2 inhibition. Through a series of experiments in cellular and fly models of HD, we show that TG2 acts in the nucleus to repress the transcription of two key metabolic genes, impeding the ability of mhtt-expressing cells to restore energy homeostasis when confronted with metabolic stress. TG2 inhibition normalizes these 'metabolic' genes and induces resistance of HD cells to mitochondrial toxins; unexpectedly this resistance was not associated with the rescue of abnormal mitochondrial bioenergetics in HD. Rather, TG2 inhibition led to normalization of gene clusters representing numerous cellular functions. These studies describe a previously unknown pathophysiological convergence between TG2 activation and transcriptional dysregulation in HD and characterize a selective inhibitor of TG2 (ZDON) as a promising, novel platform for the development of therapeutics for HD.

RESULTS

TG2 inhibition by either ZDON or genetic deletion increases mRNA of PGC-1α and cytochrome *c*

Interest in TG2 as mediator of HD pathophysiology has garnered increasing support via observations from several labs (all working in diverse models of HD that range from cells to non-human primates), that cystamine, a low molecular weight inhibitor of TG2, is neuroprotective (Karpuj et al, 2002; Fox et al, 2004). Indeed, cystamine alleviates symptoms and increases lifespan when administered to HD model mice by intraperitoneal injection or by dosing their drinking water (Bailey & Johnson, 2006; Dedeoglu et al, 2002; Van Raamsdonk et al, 2005). However, a strong and recurrent confound in the interpretation of these studies is that cystamine has numerous TG2-independent protective effects within cells (Jeitner et al, 2005), including caspase inhibition (Bailey & Johnson, 2006; Jeitner et al, 2005). Like TG2, caspases have an active site cysteine, which is essential for their proteolytic functions. Cystamine possibly acts to inhibit caspases or TG2 by forming a mixed disulfide within the active site cysteine, thus impairing their respective functions. Moreover, cystamine, acting via mechanisms that are still obscure, increases levels of the versatile antioxidant glutathione, providing another rational mechanism for its salutary effects in HD (Mao et al, 2006), where oxidative stress has been well documented (Browne & Beal, 2006). To better examine the biological role of TG2 in HD, we needed a much more selective TG2 inhibitor (Supporting Information Table S1). ZDON, a novel peptide-based irreversible TG inhibitor, fulfils this requirement in several respects. The sequence Z-QVPL (herein referred as ZDON) was discovered in Zedira GmbH, using a peptide screening approach of over 60 peptides. The strategy the company used was to mimic the gluten peptides containing a QLPF or QLPY sequence. These peptides are highly expressed in celiac patients and they have been shown to be good substrates for TG2 (TG2 is implicated in Celiac disease). ZDON mimics the gluten peptide with a DON (6-diazo-5-oxo-norleucine) core. The active site Cys residue of TG2 nucleophilically attacks DON, resulting in a stable thioether adduct. ZDON has an IC_{50} of 150 nM for recombinant TG2 (Supporting Information Fig S2). ZDON also inhibits other TG isoforms (1 and 3), although the IC_{50} for these isoforms is higher (not shown). We verified the ability of ZDON to inhibit semi-purified guinea pig TG2 in a test tube and TG activity in an established cellular model of HD: immortalized striatal cells generated from the *HdhQ111* knock-in mice ($STHdh^{Q111}$ cells bear a full-length htt with an expanded polyQ tract of 111 CAG repeats; herein after referred to as Q111) using a recently described dot blot assay (McConoughey et al, 2009). Control cells were generated from the wild-type littermate mice expressing full-length wild-type htt ($STHdh^{Q7}$, herein after referred to as Q7) (Cattaneo & Conti, 1998; Cui et al, 2006; Trettel et al, 2000). Using this TG2 activity assay, we found that 50 μM ZDON reduced the specific activity of recombinant guinea pig TG2 by 95% within 30 min and by 75% in intact immortalized striatal neurons in both Q7 and Q111 cell lines (McConoughey et al, 2009). To confirm the specific actions of ZDON, a structurally similar compound (Zc) that lacks the diazo group, which determines the reactive properties of ZDON (Supporting Information Fig S1, reactive group circled), was found to have no TG2 inhibitory activity in parallel assays. Additionally, we verified that, unlike the prototypical TG2 inhibitor cystamine, ZDON does not inhibit caspase-3 activity (Supporting Information Table S1 and Fig S3), nor does it increase glutathione levels under conditions of cellular cystine deprivation (Supporting Information Table S1 and Fig S4). These data, along with the IC_{50}s for inhibition of various TG isoforms in a test tube, suggest that at the concentration of ZDON (50–100 μM) used in intact cells, we were likely inhibiting other TG besides TG2. Nevertheless, the effects of ZDON on TG2 are more selective than previously used inhibitors (*e.g.* cystamine).

With a selective TG inhibitor in hand, we were able to explore the possibility that TG2 activity in HD contributes to the transcriptional dysregulation of metabolic genes. mhtt has been shown to inhibit the interactions of CREB and transcription initiation factor TFIID subunit 4 (TAF4) to reduce expression of genes involved in metabolic adaptation such as PGC-1α (Cui et al, 2006), a transcriptional coactivator that induces the expression of a number of genes, including cytochrome *c*, to compensate for metabolic stress (Herzig et al, 2000). Moreover, germline deletion of PGC-1α in mice confers an increased sensitivity to mitochondrial toxins and reactive oxygen species (St-Pierre et al, 2006), and produces a striatal degeneration that is very reminiscent of HD (Liang & Ward, 2006; Lin et al, 2004). We therefore examined whether TG2, an enzyme previously thought to influence mostly cytosolic events in HD, is necessary for repression of PGC-1α and/or cytochrome *c*.

Using quantitative real time PCR (RT-PCR), we established that levels of PGC-1α and cytochrome *c* were indeed lower in Q111 immortalized striatal cells than in Q7 cells (by 80 ± 3% lower for PGC-1α and 40 ± 5% lower for cytochrome *c*; Fig 1A and B). In contrast to this, the inhibition of TG2 activity, using 50 μM ZDON, resulted in increased PGC-1α mRNA levels in both Q7 and Q111 cells, by 4.5-fold and 3-fold (450 and 300%), respectively (Fig 1A). Q7 and Q111 cells treated with the structurally similar but inactive analogue of ZDON, Zc, showed no change in PGC-1α mRNA levels (Fig 1A). Like PGC-1α, cytochrome *c* mRNA levels, mildly reduced in Q111 cells relative to Q7 neurons, were increased threefold (300%) upon TG2 inhibition with ZDON (Fig 1B); as expected, Zc had no effect on the expression level of cytochrome *c* (Fig 1B). These data indicate that TG2 inhibition allows the de-repression of PGC-1α, a transcriptional coactivator of genes also involved in mitochondrial biogenesis. As expected from these findings, TG2 inhibition also derepresses transcription of a gene involved in mitochondrial biogenesis and function, cytochrome *c*, whose transcription can be enhanced by PGC-1α protein. To demonstrate that restoration of cytochrome *c* and PGC-1α transcription by ZDON is due to its TG2 inhibitory function, we examined cytochrome *c* and PGC-1α mRNA levels following TG2 knock down by small interfering RNA (siRNA). Q111 cells transfected with any one of three unique siRNAs targeted to TG2 (70–80% reduction post-transfection, not shown), resulted in an increase in both cytochrome *c* and PGC-1α mRNA levels

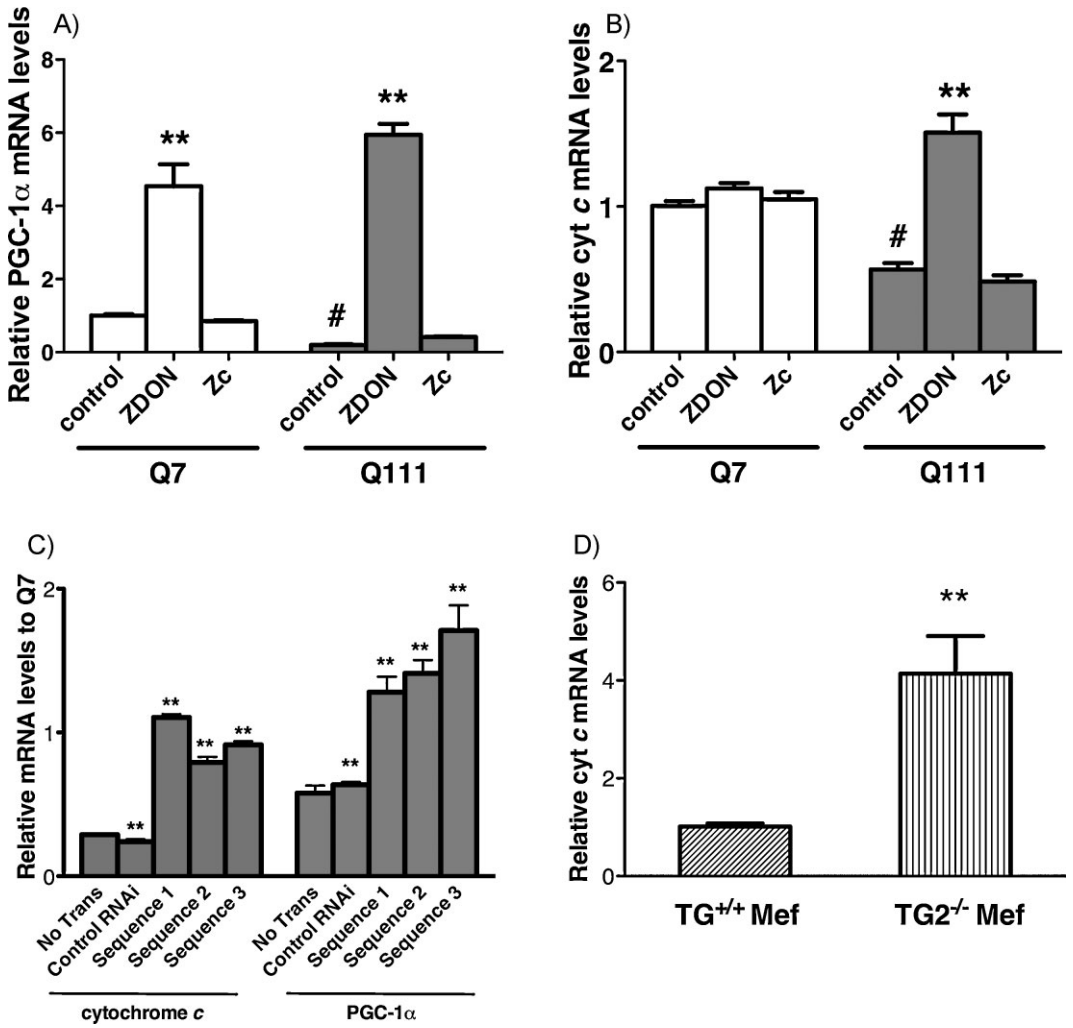

Figure 1. TG2 regulates the expression of PGC-1α and cytochrome *c*.

A. Basal levels of PGC-1α mRNA are lower in immortalized striatal cells bearing mhtt with 111 CAG repeats (Q111) than in striatal cells bearing WT htt (Q7 cells) in accordance with prior studies. ZDON treatment increases PGC-1α mRNA levels in both Q7 and Q111 cells, while the catalytically inactive Zc has no effect.

B. Following the reduction in the expression of coactivator, PGC-1α, the nuclear encoded, mitochondrial gene, cytochrome *c* is diminished in Q111 cells. ZDON treatment of Q111 cells restores cytochrome *c* mRNA levels.

C. Three unique siRNA sequences targeted against TG2 (sequences 1–3) augmented cytochrome *c* and PGC-1α mRNA levels in Q111 cells at 24–48 h post-transfection relative to no transfection (No Trans) or scrambled siRNA (Control siRNA). The qualitatively similar result between distinct treatment groups indicates that the effect is target specific and not sequence specific. Each siRNA sequence reduced TG2 mRNA levels by greater than 70% (data not shown).

D. As expected from our ZDON and siRNA studies, mouse embryonic fibroblasts (MEFs) derived from a homozygous ($TG2^{-/-}$) mouse contain higher levels of cytochrome *c* mRNA than those derived from a WT mouse ($TG2^{+/+}$ MEF).

* Denotes a $p < 0.05$ and ** denotes a $p < 0.01$; # or ## denotes a $p < 0.05$ or <0.01 when Q111 is compared to Q7.

(Fig 1C). To further support this finding, cytochrome *c* levels were examined in mouse embryo fibroblasts (MEFs) containing a germline homozygous deletion of TG2 ($TG2^{-/-}$ MEF). Compared to wild-type MEF controls ($TG2^{+/+}$ MEF) $TG2^{-/-}$ MEFs had an almost fourfold higher cytochrome *c* mRNA level (Fig 1D). Importantly, treatment with the TG2 inhibitor, ZDON, did not further increase cytochrome *c* mRNA in $TG2^{-/-}$ MEFs, supporting the notion that ZDON modulates cytochrome *c* transcription by inhibiting TG2 and not via some off-target effect (Supporting Information Fig S5). Together, these findings demonstrate that TG2 inhibition de-represses transcription of PGC-1α and cytochrome *c*, two genes critical for metabolic adaptation. Moreover, our data suggest a role for TG2 in gene silencing that does not depend on the presence of mhtt, but that is heightened by its presence (Fig 1).

Transglutaminase 2 must localize to the nucleus to repress transcription of PGC-1α and cytochrome *c*

TG2 is a protein that is distributed in multiple subcellular sites. While its cytosolic function is the best characterized, it

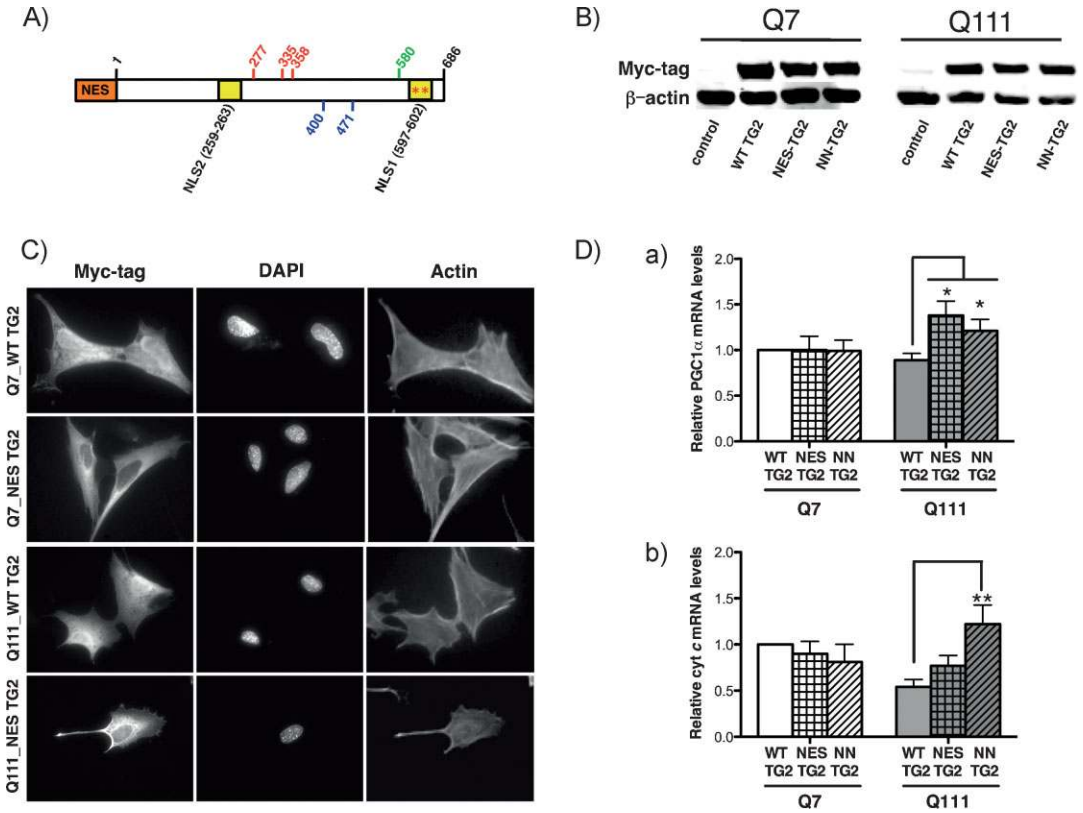

Figure 2. Nuclear TG2 is necessary to repress the transcription of PGC-1α and cytochrome *c*.

A. Schematic representation of distinct motifs within the human TG2 sequence heterologously expressed in Q7 and Q111 cells. In order to exclude TG2 from the nucleus, a nuclear export sequence (NES) was introduced at the N-terminal (NES TG2). Additional point mutations were generated in NLS1 (NN TG2). In red, three important amino acids of the transamidating domain; in blue, calcium binding sites; in green, guanine–nucleotide binding site.

B. Total lysates from Q7 and Q111 cells transfected with WT TG2, or associated NES and NLS mutants. The level of expression is similar in all the samples. β-Actin is used as a loading control. The gel is representative of at least three replicates.

C. Immunofluorescence staining shows that WT TG2 is expressed in the cytoplasm and nucleus. NES TG2 is primarily expressed in the cytosol, as predicted. Biochemical studies verified the reduced nuclear localization of TG2 with NES addition alone or NES addition plus the NLS 1 mutation (see Supporting Information Fig S6).

D. Overexpression of NES TG2 and NN TG2 increases the mRNA levels of PGC-1α and cytochrome *c* genes, compared to WT TG2 in mhtt expressing cells. The results are normalized to WT TG2 expressed in Q7 ($n = 6$); $^{*}p < 0.05$ and $^{**}p < 0.01$.

possesses canonical nuclear localization motifs and is found in the nucleus (Lesort et al, 1998). To understand if TG2 acts in the nucleus to regulate transcription of cytochrome *c* and PGC-1α, we created two TG2 mutants incapable of being targeted to the nucleus. TG2 possess two nuclear localization sequences and interacts with importin a3 (Peng et al, 1999). Amino acid residues 597–602 in human TG2 are 100% identical to residues 203–209 of the nuclear localization sequence 1 (NLS1) of the NS1 virus protein. Residues 259–263 are 80% identical to residues 34–38 of the NLS2 of the NS1 virus protein (Fig 2A). We mutated one or both of these residues; however, the mutation proximal to the catalytic core (NLS2) inactivated TG2 transamidating activity (data not shown). In order to establish the role of subcellular localization in TG's activities, we felt it was necessary to preserve TG2 activity in directing TG2 out of the nucleus. Accordingly, we inserted a nuclear export sequence from the HIV reverse transcriptase gene (Fischer et al, 1995) to the N terminal of TG2 (NES TG2-Myc) in addition to mutating its NLS1 sequence (NN TG2-Myc). We verified that all the variants generated are expressed at protein levels similar to wild type (WT) TG2 in Q7 and Q111 cells (Fig 2B) and they all retain their transamidating activity (Supporting Information Fig S6B). NES TG2 and NN TG2 are mainly localized in the cytosol as shown in the representative immunofluorescence micrographs (Fig 2C) using an antibody to the Myc-Tag to detect only the heterologous protein. Similar subcellular distribution of the heterologously expressed mutants (NES TG2-myc and NN TG2-myc) was observed following subcellular fractionation of populations of transfected cells and immunoblotting using the Myc tag antibody (Supporting Information Fig S5A).

As expected, overexpression of NES TG2 and NN TG2 (which do not target to the nucleus) increased PGC-1α and cytochrome *c* expression in Q111 cells (Fig 2D). Of note, NN TG2 was more effective in upregulating cytochrome *c* message levels, suggest-

ing that the additional NLS mutation may further reduce the amount of TG2 interacting and or modulating the transcription of this gene.

Transglutaminase 2 regulates the promoter activity of cytochrome *c*

Our studies with the TG2 mutants demonstrated that the enzyme must be in the nucleus in order to inhibit message levels of PGC-1α or cytochrome *c*. Both of these genes have been implicated in energy homeostasis either by acting as a coactivator of genes involved in mitochondrial biogenesis and fatty acid metabolism (PGC-1α) (Puigserver & Spiegelman, 2003) or by acting as an electron carrier in oxidative phosphorylation (cytochrome *c*) (Herzig et al, 2000). To further evaluate the mechanism by which nuclear TG2 silences message levels of genes involved in mitochondrial function, we took advantage of a well-established paradigm for creating energetic stress (a discrepancy between energy demand and supply) in cells. Specifically serum starvation (1–3 days) followed by serum stimulation creates an energetic demand fulfilled, in part, by increased transcription of the nuclear-encoded mitochondrial gene cytochrome *c* (Herzig et al, 2000). We transiently transfected the Q7 and Q111 immortalized striatal neurons with a promoter–reporter construct containing 326 bases of the proximal cytochrome *c* promoter fused to luciferase (-326-luc, a generous gift from Dr. Richard Scarpulla) (Fig 3A). Serum stimulation increased cytochrome *c* reporter activity over fivefold in Q7 striatal neurons ($532 \pm 10\%$ at 48 h starvation) and, as expected, to a lesser extent ($372 \pm 13\%$) in Q111 neurons (Fig 3B). In parallel experiments we co-transfected the cytochrome *c* promoter–reporter construct with cDNA for either WT TG2 or a catalytically inactive TG2 mutant (C277S) into the immortalized striatal neurons. Q111 cells were unable to induce cytochrome *c* following 48 h serum starvation followed by restimulation (100% inhibition seen in Fig 3C) while the Q7 cells showed a significant impairment in cytochrome *c* induction in the presence of overexpressed WT TG2 (Fig 3C). Inhibition of the cytochrome *c* promoter activity was greatly reduced with co-transfection of the C277S form of TG2 that has no transamidation activity; these data suggest that transamidation is required for the predominance of TG2's abilities to repress transcription. This model receives further support from the fact that addition of ZDON, which targets the transamidating activity of endogenous TG2, resulted in a 250% increase in cytochrome *c* promoter activity in Q111 cells grown in normal serum containing media (Fig 3D). A 66 base, inactive fragment (lacking the CRE and NRF-1 sites, but containing the Sp1 sites) did not respond to serum stimulation or ZDON treatment (not shown). Our studies confirmed the necessity of the CRE and NRF-1 sites to increase cytochrome *c* promoter activity in response to energetic stress, and supported the idea that ZDON affects the transcription of cytochrome *c* at the promoter level by acting via the CREB or NRF-1 sites. These results are in agreement with the hypothesis that TG2 inhibition can enhance cytochrome *c* and PGC-1α levels, in part, by promoting and/or regulating their transcription.

TG2 localizes to the cytochrome *c* promoter and to the PGC-1α gene

We showed that TG2 acts in the nucleus to repress transcription of genes silenced in a HD model (Figs 1–3). To establish whether TG2 localizes to promoters of genes that it can regulate, we performed chromatin immunoprecipitation assays (ChIPs) using an antibody specific for TG2. In these assays, Q111 cells showed almost 10 times more TG2 at the cytochrome *c* promoter than did Q7 cells (Fig 3E). ZDON treatment dramatically reduced these levels, to less than those found in Q7 cells (Fig 3E). Although ZDON also slightly increased the TG2 levels at the cytochrome *c* promoter in Q7 cells, this increase was not statistically significant. These studies are the first to localize nuclear TG2 to the promoter of an affected gene in HD. To verify the specificity of our TG2 antibody, we performed parallel ChIPs in mouse embryo fibroblasts derived from WT and $TG2^{-/-}$ animals. As expected, we detected no TG2 at the cytochrome *c* promoter in $TG2^{-/-}$ fibroblasts (Fig 3E). We also found higher steady-state levels of cytochrome *c* message in the $TG2^{-/-}$ fibroblasts, consistent with a role for TG2 as a negative regulator of its expression (Fig 1D).

PGC-1α is a coactivator that can act in concert with CREB, NRF-1 and Sp1 to enhance cytochrome *c* expression. Coactivators act in a number of ways including linking transcription factors with the basal transcriptional machinery (RNA PolII) to stimulate transcription. We investigated if TG2 was localized to the proximal PGC-1α promoter or in coding regions of the gene. In fact, coding regions of PGC-1α have previously been shown to be dysregulated by mhtt (Cui et al, 2006). While we could not find an increase in TG2 occupancy in the proximal promoter of PGC-1α (near the CRE sites), we observed fivefold greater TG2 occupancy at the boundary region of intron 2 and exon 3 in the Q111 (Fig 3F) compared to Q7 cells. This increase in TG2 parallels a decrease in RNA PolII occupancy at this site seen in R6/2 mice (Cui et al, 2006). As expected, ZDON treatment significantly reduced TG2 occupancy at this site back to Q7 levels. Of note, when TG2 mutants (NES TG2 and NN TG2) were overexpressed in Q111 cells and their ability to bind PGC-1α gene was compared to that of WT TG2 in Q111 cells, a relevant decrease in their occupancy was observed (Supporting Information Fig S6C).

Altogether, these results show that in the presence of mhtt, TG2 is localized to the proximal promoter of the cytochrome *c* gene and to the coding region of PGC-1α gene and that TG2 inhibition displaces it from chromatin and relieves transcriptional inhibition mediated by mhtt in Q111 cells. These findings support the hypothesis that nuclear TG2 directly binds to chromatin and functions as a selective corepressor of transcription of genes involved in mitochondrial adaptation in a cellular model of HD.

To determine whether the effects of ZDON reflect a reversal of a primary effect of mhtt, we used SH-SY5Y human neuroblastoma cells that express an expanded polyQ repeat (Q103) under the control of a doxycycline inducible promoter in proliferating cells. The induction of mhtt in human cells decreased the amount of PGC-1α and cytochrome *c* mRNA by approximately 50 and 10%, respectively, within 24 h of mhtt induction

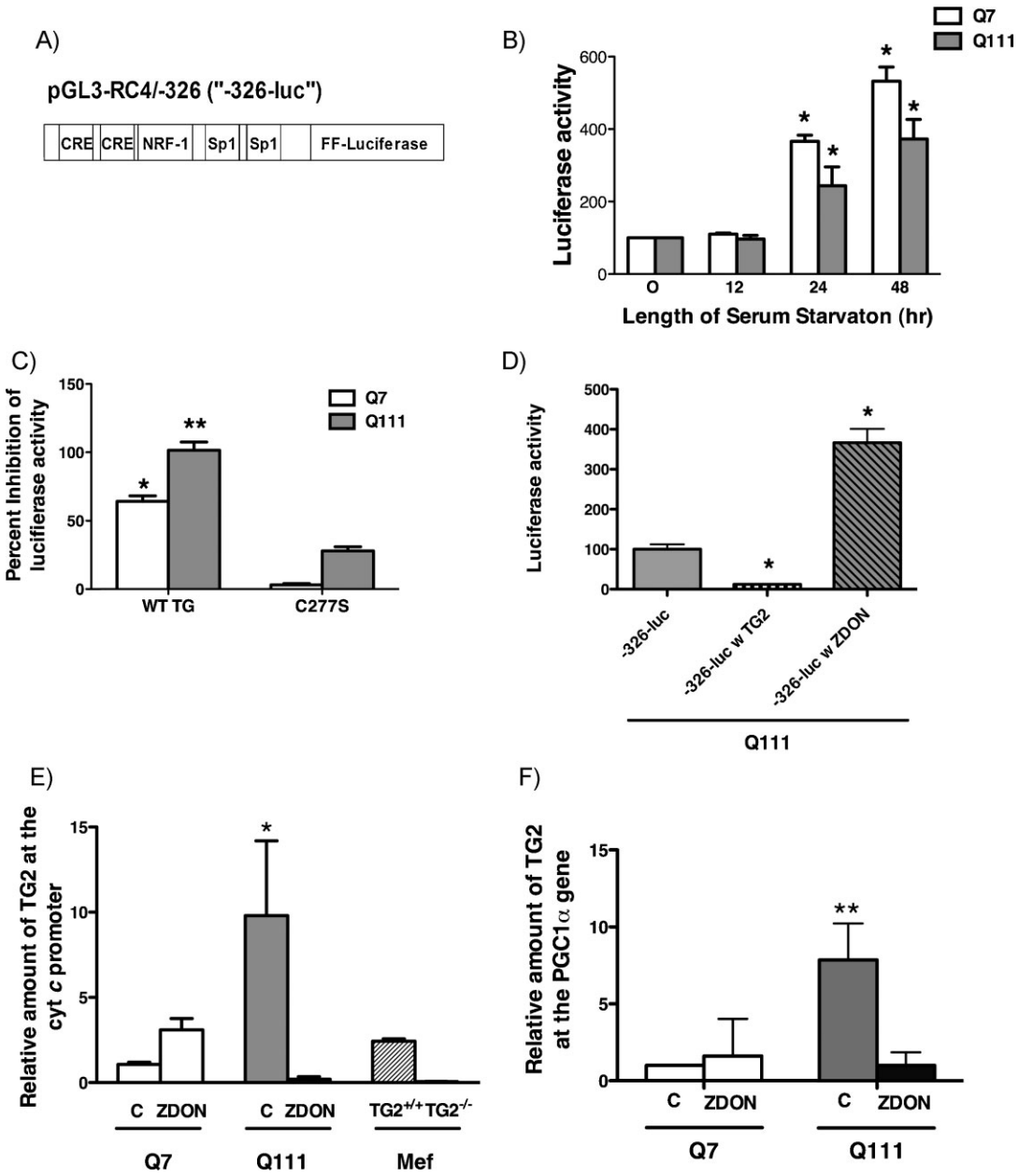

Figure 3. TG2 levels and activity influence the activity of the cytochrome *c* promoter.

A. A cytochrome *c* promoter–reporter construct that contains the proximal 326 bp of the cytochrome *c* promoter (-326-luc), including response elements for specificity protein 1 (SP1), cAMP (CRE) and nuclear respiratory factor 1 (NRF-1).

B. Q7 and Q111 cells transfected with the -326-luc construct followed by various durations of serum starvation and restimulation (serum re-addition). A more robust response of cytochrome *c* promoter activity is induced within Q7 cells (white bars) than Q111 cells (grey bars) relative to control condition (C) of no serum starvation. These findings indicate that that homeostatic response to energetic stress is repressed in cells expressing mhtt.

C. Co-transfection of a WT TG2 construct with the cytochrome *c* promoter–reporter greatly inhibited promoter activity in Q7 and Q111 cells compared to cells that were transfected with GFP and the cytochrome *c* promoter–reporter. Similarly, a TG2 construct that does not retain cross-linking activity (C277S) lost the ability to repress the cytochrome *c* promoter activity in Q7 or Q111 cells. WT and mutant TG2 were expressed at the same protein levels in these experiments.

D. Inhibition of TG activity by ZDON (50 μM for 12 h) increased the cytochrome *c* -326 promoter–reporter activity in Q111 cells nearly fourfold over non-treated cells (-326-luc w ZDON). Over-expression of TG2 repressed the promoter activity (-326-luc w TG2).

E, F. Chromatin immunoprecipitation assays showed that more TG2 is located at the cytochrome *c* promoter (E) and at the PGC-1α gene (F) in non-treated Q111 cells compared to non-treated Q7 cells. TG2 occupancy was sharply decreased in Q111 cells treated with ZDON in both cases. TG2 was found at the cytochrome *c* promoter of WT MEFs ($TG2^{+/+}$ MEF) but not in MEFs derived from $TG2^{-/-}$ cells ($TG2^{-/-}$ MEF), confirming the specificity of the TG2 antibody used for ChIP assays. The data representing each sample is normalized with respect to both IgG immunoprecipitations and input.

$^{*}p < 0.05$ and $^{**}p < 0.01$.

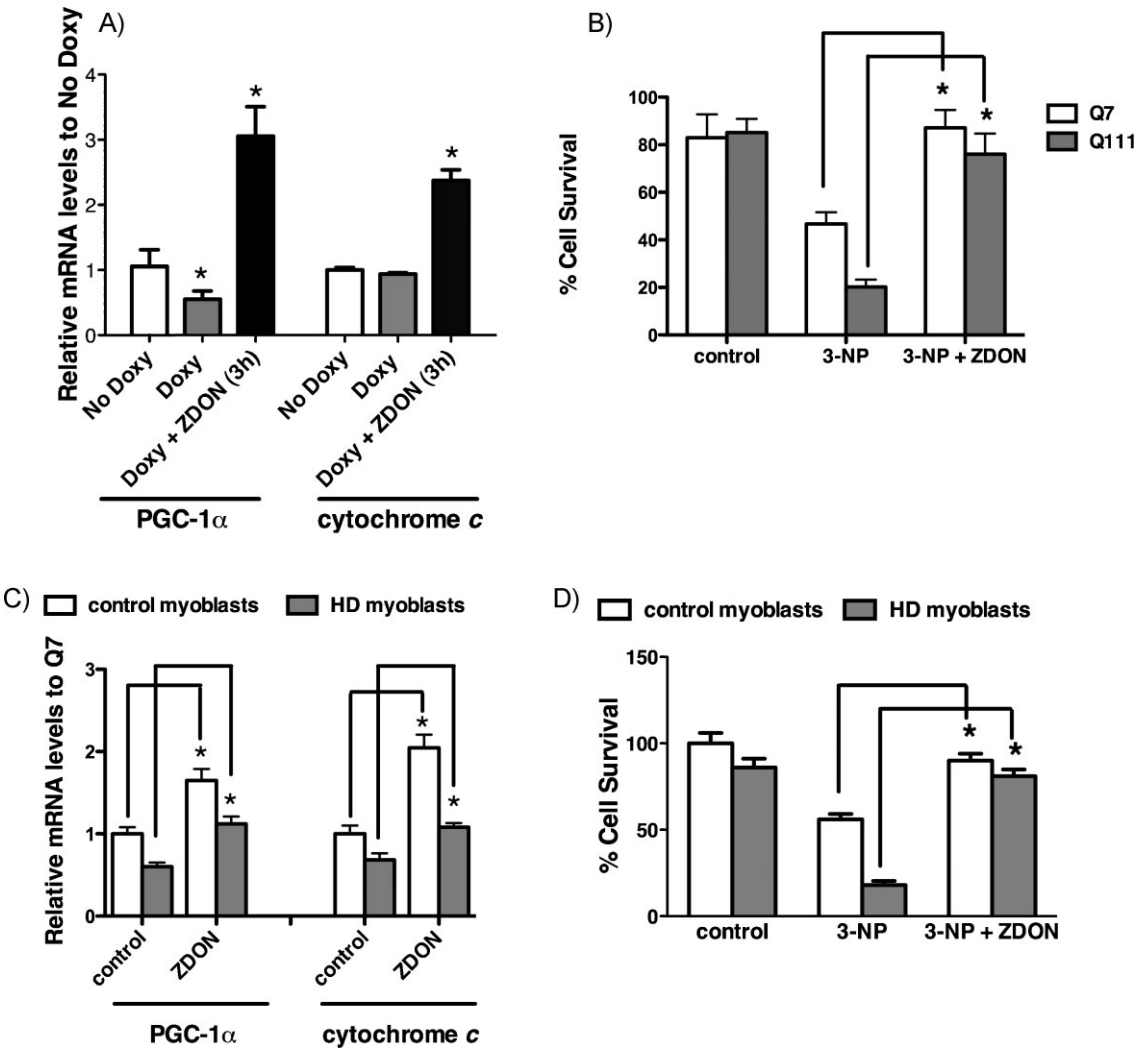

Figure 4. TG2 inhibition upregulates PGC-1α and cytochrome *c* transcription in an mhtt-dependant way and it protects immortalized striatal neurons and human myoblasts against 3-NP-induced mitochondrial toxicity.

A. Induction of mhtt by the addition of doxycycline decreased the amount of PGC-1α mRNA in human neuroblastoma cells. This decrease was reversed by 50 μM ZDON. These results demonstrate that silencing of PGC-1α expression occurs very early following mhtt expression, and is not a distal secondary or tertiary effect of chronic mhtt expression. Similarly, TG2 inhibition can nullify these proximate effects of mhtt on gene expression.

B. Q7 and Q111 cells were protected from 3-NP toxicity (10 mM for 48 h) by pre-treatment with ZDON (50 μM for 12 h). 3-NP inhibits SDH (a TCA cycle and mitochondrial respiratory chain enzyme) to induce death. Note that in agreement with prior studies, Q111 cells are more vulnerable to 3-NP than Q7 cells.

C. ZDON (50 μM for 2 h) increased the relative amount of PGC-1α and cytochrome *c* mRNA in both WT human myoblasts and myoblasts derived from HD patients. In accordance with our model, the ZDON-induced protection is highly correlated with reversal of transcriptional dysregulation in HD.

D. ZDON (50 μM for 12 h) protected myoblasts from WT and HD patients against 3-NP toxicity. These findings suggest that ZDON prevents vulnerability induced by mhtt in a human context.

$^{*}p < 0.05$.

(Fig 4A). The treatment of these cells with ZDON for 3 h resulted in the transcriptional upregulation of the expression of PGC-1α and cytochrome *c* in accordance with the results previously described (Fig 1A and B).

Transglutaminase 2 protects against 3-NP toxicity

One line of evidence pointing to the role of metabolic stress in HD pathogenesis is the ability of the metabolic toxin 3-nitropropionic acid (3-NP) to mimic several features of the disease (Beal et al, 1993). We therefore examined whether ZDON can protect Q7 or Q111 cells against 3-NP toxicity (Bailey & Johnson, 2006; Borrell-Pages et al, 2006; Dedeoglu et al, 2002; Mastroberardino et al, 2002; Van Raamsdonk et al, 2005). 3-NP is an inhibitor of both TCA cycle genes and mitochondrial oxidative phosphorylation. It is used to model selective vulnerability of the striatum to metabolic stress in WT animals,

and has been shown to be more toxic to Q111 cells than to Q7 cells (Ruan et al, 2004), an observation that we confirmed (Fig 4B). Thus, Q7 and Q111 cells were pre-treated with 50 μM ZDON for 12 h and followed by exposing them to 3-NP. After 48 h, the effects of ZDON on viability were evaluated. Pre-treatment with ZDON almost completely protected both cell lines, as measured by the calcein AM/ethidium homodimer, LIVE/DEAD assay. We verified that ZDON has no direct effect on mitochondrial bioenergetics or antioxidant defences in isolated mitochondria (Supporting Information Fig S7). These studies are consistent with a model in which ZDON protects mhtt expressing cells from a mitochondrial toxin via normalization of mitochondrial gene expression.

To further establish the ability of ZDON to ameliorate silencing of genes in a human context, we examined the effects of ZDON in human myoblasts derived from patients diagnosed with HD (Chaturvedi et al, 2009). As expected, an enhanced expression of PGC-1α and cytochrome *c* in HD myoblasts was detected by following treatment with ZDON (50 μM for 2 h) (Fig 4C). Normalization of gene expression was again associated with resistance to 3-NP toxicity (Fig 4D). Altogether, these studies establish the ability of ZDON to reverse the vulnerability to mitochondrial toxins created by mhtt expression in rodent and human cells.

Metabolic biomarkers after TG2 inhibition

To establish whether TG2 inhibition not only normalizes metabolic gene expression, but also augments mitochondrial function and mass, we measured several biomarkers of mitochondrial metabolism in Q111 cells: citrate synthase (CS) activity, ND6 protein levels and mitochondrial membrane potential (Fig 5). We also performed bioenergetic studies in isolated mitochondria (Supporting Information Fig S8). Citrate synthesis is the first step of the TCA cycle and citrate is produced from pyruvate to enter the mitochondria in the form of acetyl Co-A; accordingly CS has been used as an indirect measure of mitochondrial number and mass. ZDON (50 μM) treatment for 24 h increased CS specific activity approximately by 50% in both the Q7 and the Q111 cells (Fig 5A). The ND6 subunit is necessary for the proper formation and function of complex I, a component of the respiratory chain (Chomyn, 2001). Although ND6 is a protein encoded by the mitochondrial genome, the transcription factors that regulate mtDNA expression are nuclear encoded (Chomyn et al, 1985, 1986). Western blot analysis and associated quantification revealed that ND6 levels were significantly enhanced in Q111 cells after 24 h exposure to ZDON (Fig 5B). Both these ZDON-induced changes (increased CS specific activity and increased ND6 levels) reflect increases in mitochondrial mass. To further evaluate the effect of ZDON on mitochondrial mass, we utilized a Mitotracker® dye that passively diffuses across the plasma membrane and accumulates in mitochondria in amounts proportional to the mitochondrial membrane potential. The membrane potential represents an electrochemical gradient, which upon dissipation via the F_1–F_0 ATPase can be converted to ATP. We measured Mitotracker® staining 12 and 24 h after treatment (50 μM ZDON). ZDON enhanced Mitotracker® staining of Q7 and Q111 striatal cells (Fig 5C and D) providing additional support for a ZDON-mediated increase in mitochondrial mass.

Studies of isolated mitochondria from Q7 and Q111 cells supported the notion that CS and other TCA cycle enzymes (SDH) are reduced by pathological polyQ expansions (not shown). However, analysis of mitochondrial bioenergetics in isolated mitochondria from Q7 with Q111 cells indicates several unexpected observations. First, while it is clear that the total number of mitochondria are reduced (likely related to clear silencing of PGC1a and cytochrome c), the oxidative phosphorylation and respiratory chain activity of each are not impaired in Q111 cells, despite clear silencing of PGC-1α and cytochrome *c* gene expression. Moreover, despite its ability to normalize PGC-1α and cytochrome *c* mRNA levels and increase mitochondrial mass, ZDON does not increase basal or maximal respiratory capacity of Q111 cells. In fact, the respiratory data indicate that mitochondria from Q111 cells are capable of higher spare respiratory capacity and higher maximum respiratory rate than their 'WT' counterparts in the absence of ZDON. Moreover, ZDON does not increase total SDH activity, although, as mentioned, it does increase CS activity (Fig 5A). The lower activity of TCA cycle enzymes (CS and SDH per total protein) and the higher-than-expected activity of mitochondrial electron transport chain enzymes (respiratory control index, V_{max}, etc., Supporting Information Fig S8) mean that Q111 mitochondria are optimized for oxidations rather than biosynthesis. Accordingly, Q111 cells are more vulnerable to TCA cycle toxins, such as 3-NP (Fig 4B) which would further reduce the ability of Q111 mitochondria to provide electrons via NADH and $FADH_2$ to the mitochondrial electron transport chain for energy generation. The increase in CS by ZDON raises the possibility that ZDON acts to improve cellular energetic status by increasing the number of mitochondria to create resistance to 3-NP. Paradoxically, we do not see a similar increase in another TCA cycle enzyme such as SDH (Fig 5A). Therefore, we cannot exclude the possibility that TG2 inhibition induces resistance to 3-NP by increasing the ability of extramitochondrial sites to generate substrates that can be used in the mitochondria. Examples of utilizable substrates from extramitochondrial sites include pyruvate (generated from lactate via actions of lactate dehydrogenase) or short chain fatty acids. Alternatively, ZDON could interfere with death signalling cascades downstream of ATP depletion. However, our isolated and cellular mitochondrial studies in Q7 and Q111 cells point to a more complicated model for ZDON-induced protection from 3-NP, which extends beyond PGC-1α cytochrome *c* and mitochondrial-based metabolic compensation. The notion that metabolic abnormalities derive from extramitochondrial rather than mitochondrial sites is not new (Lee et al, 2007).

Transcriptome analysis following TG2 inhibition reveals selective upregulation of several classes of genes

While TG2 inhibition leads to increased expression of genes that drive mitochondrial mass, the unexpected lack of increased respiratory function or capacity per mitochondria by ZDON raises the possibility that other genes might be regulated by TG2

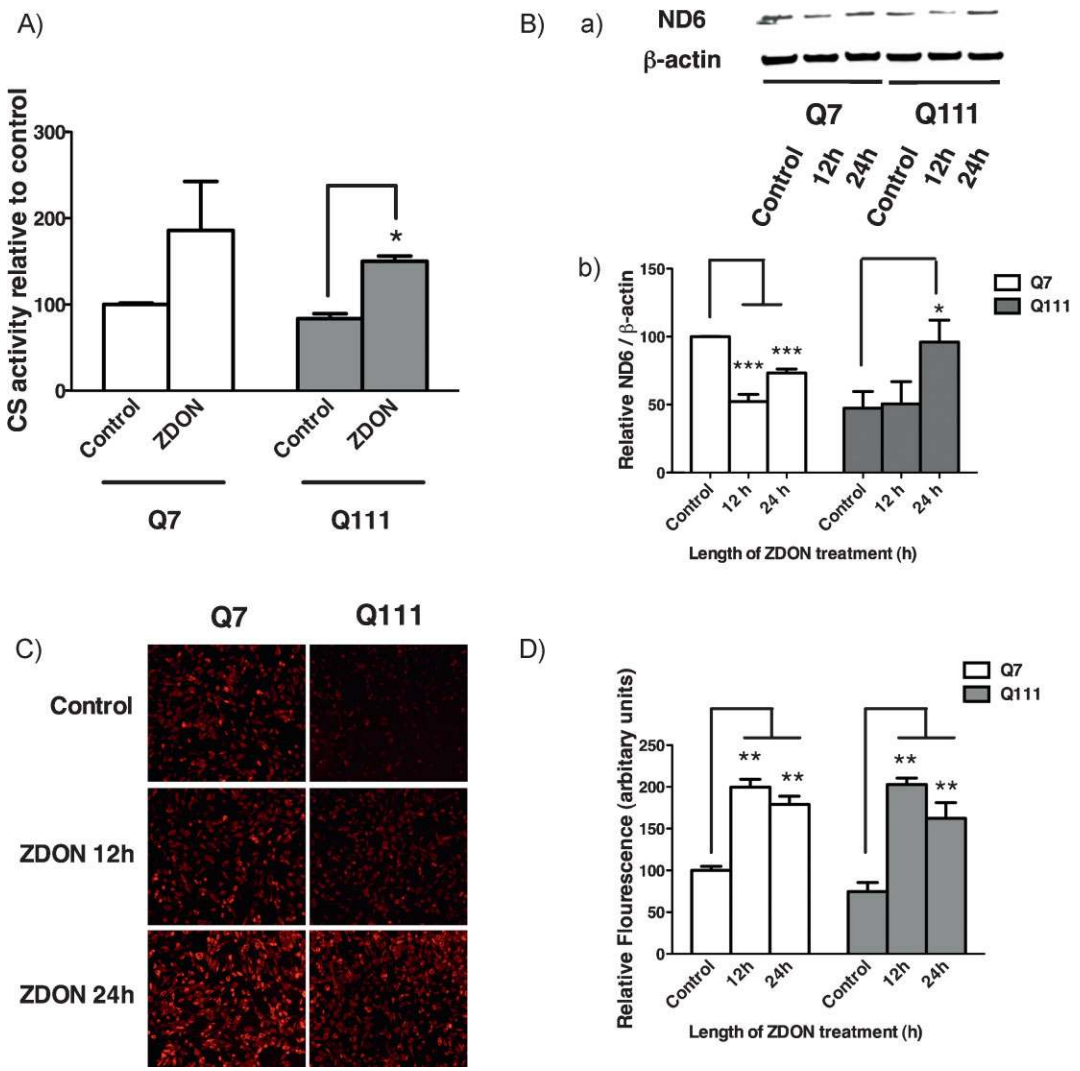

Figure 5. TG2 inhibition by ZDON increases markers of mitochondrial mass (A), nuclear encoded mitochondrial protein expression (B) and increases mitochondrial membrane potential (C, D) but does not improve mitochondrial bioenergetics in isolated mitochondria (Supporting Information Fig S8).

A. CS specific activity was increased after 24 h of ZDON treatment. CS is the enzyme that converts pyruvate to Acetyl-CoA is an accepted marker of mitochondrial mass (Chavez et al, 2010).

B. ND6 was increased relative to β-actin in Q111 cells after 24 h treatment of ZDON. Nuclear encoded mitochondrial transcription factor A (Tfam) is a PGC-1α regulated gene. Tfam, in turn, acts in the mitochondria to induce ND6 expression. The induction of ND6 by ZDON is consistent with ZDON-induced increases in PGC-1α expression and activity.

C. Mitotracker® staining was increased in both Q7 and Q111 cells after ZDON treatment. Mitochondrial mass is increased by ZDON in both Q7 and Q111 cells. According to the bioenergetic studies the increase in membrane potential could reflect an increase in the biosynthetic capacity of respiratory chain substrates by mitochondrial (TCA cycle) or extramitochondrial sites (pyruvate, fatty acids) by ZDON.

D. Quantification of Mitotracker® staining with and without the addition of ZDON (50 μM for 12 h).

$^{*}p < 0.05$ and $^{**}p < 0.01$.

inhibition to account for the resistance to metabolic stressors such as 3-NP. We also were interested in establishing the specificity of gene changes induced by ZDON in Q7 versus Q111 cells. To begin to address these questions, we performed microarray analysis on RNA purified from Q7 and Q111 immortalized striatal cells, before and after treatment with ZDON. We also tested two additional, structurally diverse TG2 inhibitors, Boc-DON, already described in literature as a specific TG2 inhibitor (Parameswaran et al, 1990) and the broad TG2 inhibitor, cystamine (Bailey & Johnson, 2006), to exclude any off target effects of ZDON. Expression of mhtt in Q111 cells induced dysregulation of 461 probes (289 upregulated, 172 downregulated, $p < 0.005$) compared to Q7 (Q111 Not Treated in Fig 6A). This profile of gene expression is similar to that found by MacDonald and colleagues in their analysis of gene expression in Q111 versus Q7 cells (microarray analysis, GEO

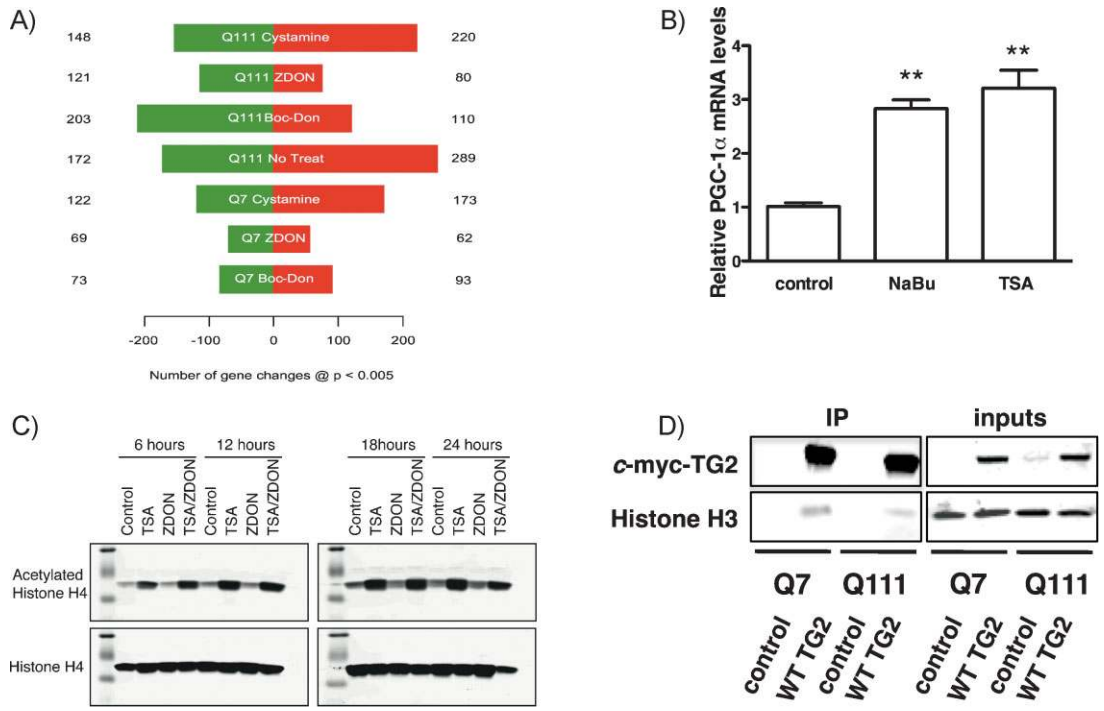

Figure 6. ZDON normalizes the expression of many genes repressed in Q111 cells and it acts independently of HDACs to enhance cytochrome *c* and PGC-1α expression levels.

A. Q111 cells have 461 dysregulated probes, relative to Q7 cells, and ZDON had a large effect (more than 40% of dysregulated genes) in normalizing this dysfunction. Ontology gene sets affected by ZDON are broad and include p53-regulated genes, glutathione metabolism genes and chaperone genes.

B. Prototypical HDAC inhibitors NaBu or TSA increased the amount of PGC-1α mRNA in Q111 cells. These findings demonstrate that ZDON induces PCG-1α mRNA expression as well as NaBu or TSA.

C. ZDON does not affect the acetylation state of H4 as measured by immunoblotting. As expected, the classes I and II HDAC inhibitor TSA increased H4 acetylation. ZDON works independent of canonical changes in histone acetylation to modify transcription. These results are congruent with an HDAC independent role for TG2 in epigenetic regulation.

$^{*}p < 0.05$ and $^{**}p < 0.01$.

D. WT TG2 interacts with Histone H3 in Q7 and Q111 cells supporting the evidence that TG2 modulates transcription. The ability of TG2 to interact with Histone H3 is consistent with a role for TG2 in modulating facultative heterochromatin formation by affecting N-terminal post-transcriptional modifications of histones, also known as the 'histone code'.

Dataset GSE21237; Lee et al, 2007). Of note, promoter analysis of the 461-dysregulated probes revealed an over-representation of Sp1 targets ($p = 0.0047$), congruent with previous reports involving Sp1 in HD pathogenesis (Chen-Plotkin et al, 2006). Ingenuity pathway analysis revealed dysregulation of networks centred on *Ppar-γ* and NF-κB (Supporting Information Fig S9). *Ppar-γ* was significantly upregulated in Q111 striatal cells, whereas *Pparc1* (PGC-1α gene) was slightly downregulated, consistent with prior reports (Fig 1A). 'transcription factor activity', 'nucleosome' and 'programmed cell death' were among the most represented gene ontology (GO) categories (Supporting Information Fig S10, microarray analysis- GEO Dataset GSE21237).

We next assessed the extent to which ZDON treatment was able to rescue the transcriptional dysregulation caused by Q111 expression. One hundred and ninety-six out of the 461 (42%) Q111-related probes showed at least a 25% shift towards normal levels (or levels in Q7 cells) after treatment with ZDON. Of these, 10 probes were completely restored to normal levels after treatment. GO analysis showed that ~40% of the genes in the top categories tended toward normalization. The structurally diverse TG2 inhibitors Boc-DON and cystamine (which both protect against 3-NP toxicity, not shown) produced a similar normalization in gene expression patterns in the mutant line (37 and 38%, respectively), but ZDON was the most effective in normalizing gene expression relative to Q7 untreated cells (Q111 ZDON *vs.* Q111 No Treat, Fig 6A). ZDON treatment at least partially reversed all the pathogenic changes observed with mhtt in histone genes, demonstrating that TG2 has a major direct effect on chromatin remodelling and transcriptional dysregulation in HD. ZDON treatment in normal Q7 striatal cells had no effect on any of these genes demonstrating the selectivity of TG2 inhibition for genes dysregulated by mhtt. Of note, ZDON also restored expression levels for one HSP40 family member, DNAJB10 ($p < 0.05$) in the microarray; increased DNAJB10 message by ZDON in Q111 cells was confirmed by quantitative real time RT-PCR (Supporting Information Fig S11). Previous studies showed that cysteamine, an FDA approved TG2

inhibitor, can also normalize DNAJB10 levels, and thus increases brain-derived neurotrophic factor (BDNF) trafficking, BDNF levels and neuroprotection in HD (Borrell-Pages et al, 2006). Altogether, our microarray analysis suggests that ZDON normalizes expression of a large subset of genes, particularly those dysregulated in HD. These findings are consistent with a model in which increased TG2 acts in the nucleus at gene promoters to dysregulate expression of metabolic, chromatin, chaperone and cell death genes in HD. The normalization of these genes by structurally diverse TG2 inhibitors in a cellular model of HD provides indirect support for increased activity of nuclear TG2 observed by numerous other groups in prior mouse and human studies (Jeitner et al, 2008; Karpuj et al, 1999, 2002).

TG2 modulates transcription independently of HDACs

The ability of TG2 inhibition to normalize so many genes in HD raised the possibility that ZDON might be acting directly or indirectly to inhibit histone deacetylases (HDACs) in normalizing transcription in rodent and human cells. HDACs are proteins that regulate transcription by acetylating N-terminal tails of histone proteins and modulating facultative heterochromatin (Sleiman et al, 2009); alternatively or in concert they act by directly modifying the acetylation states of transcription factors or coactivators to recruit the basal transcriptional machinery (Ryu et al, 2003). To verify that ZDON is not acting as an HDAC inhibitor, we compared its effects on histone acetylation to canonical HDAC inhibitors.

HDAC inhibitors are known to reverse transcriptional silencing in HD and to protect striatal neurons expressing mutant htt from a host of stresses (Steffan et al, 2001). Sodium butyrate (NaBu, a class I HDAC inhibitor) and Trichostatin A (TSA, an inhibitor of class I and II HDACs) regulated the cytochrome *c* promoter–reporter levels to an extent similar to that exhibited by ZDON (data not shown), and these compounds also increased the mRNA levels of PGC-1α (Fig 6B). Histone H4 acetylation, which is associated with a transcriptionally active conformation of chromatin, was increased by HDAC inhibitors and was unaffected by ZDON (Fig 6C). Moreover, ZDON and HDAC inhibitors in combination did not alter global H4 acetylation levels as compared to HDAC inhibitors alone. These findings suggest that TG2 inhibition acts independently of HDAC inhibition to reverse transcriptional repression of PGC-1α and cytochrome *c* in an HD model.

If TG2 inhibition acts independently of histone acetylation, how is TG2 then binding to chromatin and modulating transcription in the presence of mhtt? One obvious possibility is that mhtt (with its abundant polyQ residues) is recruiting TG2 (an enzyme which crosslinks glutamines and lysines or polyaminates glutamine residues) to relevant promoters to silence (or augment) gene expression. However, co-immunoprecipitation experiments using antibodies to full-length mhtt or N-terminal fragment of mhtt failed to identify any TG2 bound to either form of the protein (Zainelli et al, 2005), nor is ZDON directly affecting mhtt levels to affect resistance to mhtt toxicity. In contrast, parallel experiments using a monoclonal antibody to Histone H3 identified a clear interaction between H3 and TG2 in the nuclei of Q111 cells (Fig 6D). These findings, which are the first to document an interaction of TG2 with histone proteins in an intact cell, are consistent with prior test tube experiments that have shown that TG2 can post translationally modify histone proteins (Ballestar et al, 1996, 2001; Ballestar & Franco, 1997). In addition, they are consistent with a model where TG2 interacts with Histone H3 to polyaminate its N-terminal tail leading to increased electrostatic interaction between positively charged histone proteins and negatively charged DNA. Inhibition of TG2 would reduce polyamination of the N-terminal of histones including Histone H3, decrease positive charge on histone proteins, reduce interaction with DNA and promote an open, transcriptionally active conformation leading to reversal of transcriptional silencing in HD.

ZDON is protective in an HD fly model

The ability of ZDON to normalize genes belonging to many GO groups predicts that ZDON should not only protect against 3-NP vulnerability but also reduce mhtt-induced neurodegeneration. ZDON is a peptide-based inhibitor, which presents obvious challenges in penetrating the blood brain barrier. To establish whether ZDON can protect against neurodegeneration induced by mhtt *in vivo*, and to avoid some of the problems associated with delivering peptides into the CNS in rodents, we examined the effect of ZDON in an established *Drosophila* model of HD (Agrawal et al, 2005; Marsh & Thompson, 2006; Steffan et al, 2001). This model has been extensively studied and expresses an exon 1 fragment of mhtt that contains a 93 glutamine repeat under control of a pan neuronal driver (*elav*, using the UAS Gal4 system) (Agrawal et al, 2005). Neuronal degeneration can be measured in this model by counting the number of surviving photoreceptor neurons as reflected by the number of rhabdomeres in each ommatidium in the eye. WT flies have seven visible rhabdomeres per ommatidium, but as HD flies age there is a loss of rhabdomere number, thus providing a readily measurable biomarker of mhtt-induced degeneration. ZDON is soluble in dimethyl sulphoxide (DMSO), which is highly toxic to the Q93 flies; therefore we conducted toxicity studies to determine the amount of DMSO-dissolved ZDON that could be tolerated by the *Drosophila* without causing overt toxicity (Fig 7B). The highest non-toxic, final concentration of ZDON in the food was found to be 125 μM, and this concentration was then tested for its ability to inhibit TG2 activity in fly head homogenates using an *in vitro* TG activity assay. *Drosophila* have only one form of TG, which contains the same catalytic triad and Ca^{2+}-binding site as TG2 but lacks the GTP-binding activity (Ikle et al, 2008). Flies fed food containing 125 μM ZDON showed an 80–90% decrease in TG activity without apparent toxicity (data not shown) and an increase in the number of rhabdomeres at 10 days of age as compared to those fed vehicle (Fig 7A). One group of control flies was given no DMSO, and another control group was given DMSO alone (approx. 0.2%) with no ZDON. There was no significant difference between the two control groups. When percent rescue was calculated with the equation: $100 \times (R_t - R_c)/(7 - R_c)$, R_t is the number of rhabdomeres/ommatidium in the ZDON group and R_c is the control group, ZDON showed a significant rescue relative to DMSO only fed flies (21%). In addition to the increase

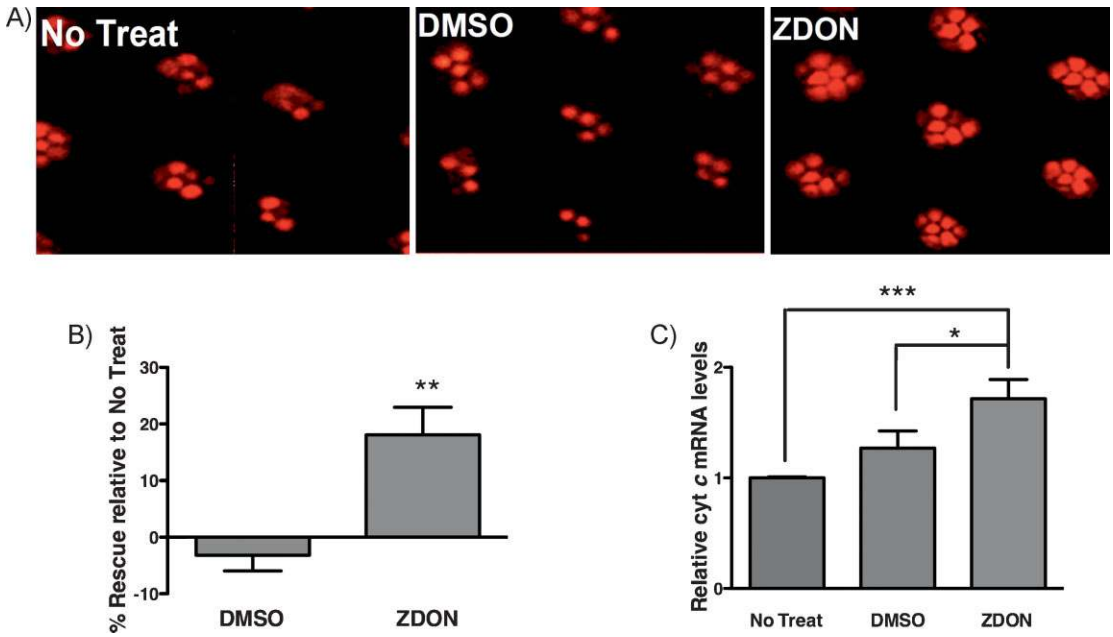

Figure 7. TG2 inhibition by ZDON is protective in a fly model of HD. The ability of ZDON to affect a broad swath of genes dysregulated by mhtt led us to test the ability of ZDON to prevent mhtt induced degeneration in photoreceptors.

A. A *Drosophila* HD model expressing exon 1 of htt with 93 CAG repeats (Q93) fed ZDON (125 μM final concentration in food) displayed a greater number of rhabdomeres per ommatidium than HD Q93 flies receiving no treatment (control) or DMSO alone (Vehicle).

B. This was calculated as a 21% rescue from DMSO and a 17% rescue from the control group by the formula: $100 \times (R_t - R_c)/(7 - R_c)$, R_t is the number of rhabdomeres/ommatidium in the ZDON group and R_c is the control group.

C. A *Drosophila* model of HD fed ZDON (125 μM final concentration in food) showed increased cytochrome *c* mRNA when compared to those that were not fed ZDON (control) or those fed only DMSO.

$^{*}p < 0.05$ and $^{**}p < 0.01$.

of rhabdomere number, ZDON fed *Drosophila* also displayed augmented cytochrome *c* mRNA levels (Fig 7C). These studies suggest that ZDON-induced neuroprotection is associated with reversal of transcriptional dysregulation in a fly model of HD.

TG2 inhibition protects from NMDA toxicity in YAC128 primary neurons

To establish whether neuroprotection from mhtt-induced neurodegeneration by ZDON can be observed in the cell type most vulnerable to degeneration in HD, we studied excitotoxic death in striatal neurons cultured from YAC128 mice. Several studies support the hypothesis that mhtt contributes to increased neuronal susceptibility to excitotoxicity, a state in which aberrant stimulation of neurons leads to their death (Heng et al, 2009; Okamoto et al, 2009; Zeron et al, 2002). N-methyl-D-aspartic acid (NMDAs) toxic effect in HD mice and cellular models has been attributed to cytosolic calcium overload or to increased mitochondrial depolarization (Browne, 2008; Fernandes et al, 2007). Furthermore, NMDA activation has been recently reported to induce repressive transcription via extrasynaptic NMDA receptors in YAC128 mice, a knock in mouse model for HD (Okamoto et al, 2009). To explore the possible involvement of TG2 in extrasynaptic glutamate mediated transcriptional repression, we pre-treated medium-sized spiny neurons (MSNs) with ZDON and its negative control Zc for 12 h, then incubated the cultures in a balanced salt solution in the presence of NMDA (500 μM). As previously reported (Graham et al, 2006), cultured YAC128 MSNs displayed increased apoptosis 24 h after NMDA exposure compared with WT MSNs (YAC128 = 31.9 ± 1.03% *vs.* WT = 21.3 ± 1%; Fig 8A and B). Interestingly, TG2 inhibition protected both WT and mutant MSNs from NMDA toxicity (YAC128 = 13.1 ± 3.4% *vs.* WT = 9.8 ± 1.4%) and its effect was more dramatic in the presence of mhtt (7% increase in protection). The use of Zc did not have any effect on NMDA toxicity (YAC128 = 27 ± 2% *vs.* WT = 21 ± 1.3%; Fig 8B).

These experiments show that TG2 inhibition protects vulnerable striatal neurons from NMDA toxicity in the presence or absence of mhtt. Given that recent studies have shown that PGC-1α is sufficient to prevent NMDA toxicity in YAC128 striatal neurons (Okamoto et al, 2009), the finding herein that TG2 inhibition is sufficient to reduce mhtt-induced repression of PGC-1α offers a logical mechanism by which ZDON is protective in this model.

DISCUSSION

Despite extensive genetic and pharmacological studies (Bailey & Johnson, 2006; Dedeoglu et al, 2002; Mastroberardino et al,

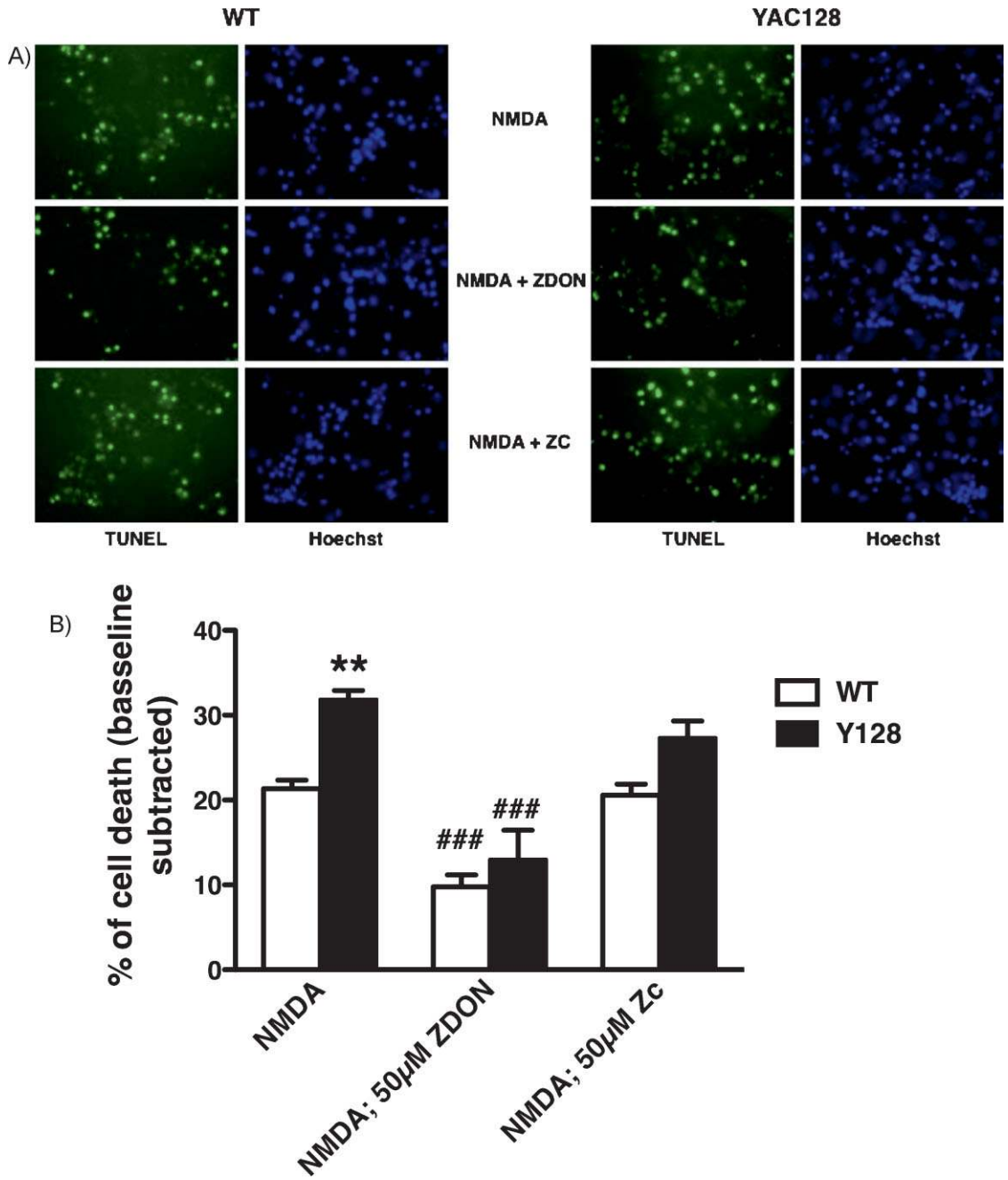

Figure 8. Effect of ZDON and control peptides on NMDA-induced toxicity in MSN cultures from WT and Y128 mice.

A. TUNEL assay (a biomarker of apoptotic death) of medium-sized spiny neurons following 24 h of NMDA exposure. The MSNs pre-incubated with ZDON (50 μM) for 12 h showed less apoptotic nuclei that the ones untreated or pre-treated with Zc (50 μM), demonstrating the protective effects of TG2 inhibition against NMDA-mediated toxicity. Extrasynaptic NMDA induces changes in cytosolic calcium sufficient to further activate TG2 and repress adaptive transcription. We propose a model whereby TG2 inhibition prevents extrasynaptic glutamate from inducing transcriptional dysregulation and leads to neuroprotection.

B. Quantification of Fig 8A.

$^{**}p < 0.01$, comparing WT to Y128; $###p < 0.001$, comparing to NMDA treatment group of its genotype.

2002; Van Raamsdonk et al, 2005), the precise mechanism(s) by which TG2 mediates deleterious effects in HD remain(s) obscure. Here, we provide evidence that TG2 participates with mhtt to induce broad dysregulation of gene expression in a well-studied and validated mouse model of HD (Q111). As expected, inhibition of TG2 by structurally diverse, low molecular weight inhibitors relieves a significant level (40%, Fig 6A) of transcriptional dysregulation and is associated with resistance

to mhtt-induced neuronal degeneration, *in vitro* and *in vivo*. We show that nuclear TG2 requires its transamidating activity to influence cytochrome *c* and PGC-1α transcription by binding chromatin and we also demonstrate an interaction between TG2 and Histone H3 in Q7 and Q111 cells. These findings are consistent with a model whereby TG2 polyaminates N-terminal tails of histones to modulate facultative heterochromatin formation and thus affects a large number of genes associated not only with nucleosomes and chromatin remodelling, but also genes related to chaperone, programmed cell death and metabolic function. Our data provide unexpected pathophysiological convergence between two previously disconnected aspects of HD pathogenesis: nuclear TG hyperactivity and transcriptional dysregulation.

Within the eukaryotic nucleus, DNA is organized by its incorporation into chromatin. The basic subunit of chromatin is the nucleosome, which is composed of DNA coiled around an octamer of histone proteins, two molecules each of histone H2A, H2B, H3 and H4. Histone H1 associates with chromatin outside the nucleosome (Sleiman et al, 2009). The amino-terminal 'tail' of each histone is evolutionarily conserved and it is target of numerous post-transcriptional modifications. Post-translational modifications of histones are major players in epigenetic control. These modifications include the acetylation, methylation, phosphorylation, ADP-ribosylation and monoubiquitination. The specific pattern of histone modification, or 'histone code', is used by proteins involved in chromatin organization to establish a transcriptionally silent or active state (Ratan, 2009). Here, we provide data supporting the idea that TG2 may catalyse polyamine addition to histones that might add additional complexity to the 'histone code'. Polyamines are organic compounds that have two or more amino groups. Alone or when covalently attached to a protein, they bind DNA readily, but unlike Ca^{2+}, their positive charge is spread evenly throughout the molecule. Their avidity for DNA on a charge basis makes them ideally suited to regulate the conformation of DNA. Attaching them to proteins (via TG2) provides an elegant way to manipulate polyamine concentrations (organic cations) locally to be able to alter propensity for DNA (highly negatively charged due to phosphate backbone) to assume a compact (silenced) conformation. By contrast, suppression of TG2 should inhibit polyamination of histone protein, thereby decreasing histone–DNA interactions and increasing gene expression. In a number of *test tube* studies, polyamination of glutamines in histone tails by TG has been shown to occur. Indeed, Ballestar (Ballestar & Franco, 1997) showed that TG2 polyaminates glutamine 5 and 19 of Histone H3 and glutamine 22 of histone 2B. Our study is the first to demonstrate an interaction between TG2 and any histone protein in an intact cell, and the first to conclusively demonstrate a role for nuclear TG2 in gene regulation. While we clearly show that TG2 inhibition works independently of HDAC inhibition to augment transcription (Fig 6D), future studies will define whether hyperpolyamination of histone tails is the mechanism by which TG2 hyperactivation in HD contributes to gene silencing in this disease.

Identification of a cassette of genes modulated by TG2 inhibition can be utilized as an *in situ* biomarker for therapeutic strategies in HD centred on the inhibition of this intriguing enzyme. Current activity measurements for TG2 only allow measurement of maximal activity (V_{max}) in a population of cells, as they involve exogenous addition of a calcium ionophore to cells in monolayer, which fully activates the enzyme (Supporting Information Fig S6B). Our gene array studies define a group of genes (*e.g.* β-actin, $p21^{waf1/cip1}$ and tp53inp1, mdm2) that are highly upregulated (7- to 30-fold) by TG2 inhibition. Consistent with prior observations of mhtt interacting with p53 (Steffan et al, 2000), three of these genes are associated with p53 upregulation ($p21^{waf1/cip1}$, tp53inp1, mdm2), particularly in p53 responses to oxidative stress. This gene cassette could reflect an augmentation of the DNA damage response by ZDON, but also could be used (via *in situ* hybridization) as a sensitive way to monitor TG2 activity in vulnerable striatal neurons in animal models of HD or in human autopsy tissue. By extension, appropriate pharmacokinetics of inhibitors of the enzyme could then be determined by assaying the point above which, the levels of this cassette of genes in the striatum of rodents expressing mhtt increase.

Our studies of TG2 involved in transcriptional silencing in HD were stimulated by observations that this enzyme regulates nodal genes in metabolic adaptation: cytochrome *c* and PGC-1α (Fig 1). The reversal of mhtt-induced silencing of both of these genes and a host of markers of mitochondrial mass and function (CS, ND6 and mitochondrial membrane potential, Fig 5) by ZDON seemed congruent with a straightforward model: TG inhibition normalizes mitochondrial biosynthetic and oxidation capacity to overcome metabolic defects in an HD striatal lines. However, detailed mitochondrial bioenergetic analyses suggest that this simple model is incorrect in Q111 cells. Indeed, mitochondrial oxidation capacity (electron transport chain activities and oxygen utilization, V_{max}) is actually increased in Q111 as compared to Q7 cells. In fact, it appears that in Q111 cells, the ability of the mitochondria to synthesize substrate for oxidation (via the activity of TCA cycle enzymes) is diminished (Supporting Information Fig S8). These data are completely congruent with the increased vulnerability of Q111 and human HD myoblasts to 3-NP, a toxin that inhibits TCA cycle enzymes (*e.g.* SDH and fumarase). However, the absence of an increase in SDH message or activity by ZDON refutes the simple notion that PGC-1α, a known coactivator of mitochondrial biogenesis, is globally increasing all TCA and respiratory chain components in response to TG2 inhibition and thus creating resistance to 3-NP. Future studies will determine the exact contribution of PGC-1α to protection by ZDON in loss of function studies. Whatever the results, these findings are consistent with prior observations from other groups that mitochondrial oxidative phosphorylation is not decreased in HD cells (Browne, 2008) and that in contrast, it is increased. The diminished mitochondrial biosynthetic capacity in Q111 cells (if extendable to rodent models and human autopsy studies) has clear therapeutic implications. Strategies to enhance substrate delivery to the mitochondrial respiratory chain (*e.g.* via feeding pyruvate, malate, NADH, $FADH_2$ or short chain fatty acids) in HD patients may feed the 'augmented mitochondrial engine' that Q111 cells possess and thus

overcome the metabolic abnormalities that characterize HD. Methods to generate ATP from extramitochondrial sites in striatal neurons are a reasonable alternatives (Lee et al, 2007). Indeed, activators of glycolytic gene expression protect Q111 cells from 3-NP toxicity (Niatsetskaya et al, 2010) and small molecules that reprogram metabolism are protective in more complex HD models (Parker et al, 2005).

The inability of ZDON to improve mitochondrial bioenergetic parameters raised questions regarding the mechanism by which TG2 inhibition protects against mhtt-induced cell dysfunction and death (Battaglia et al, 2007). We excluded the possibility that ZDON (like cystamine or cysteamine) could directly inhibit caspases or increase glutathione levels to mediate protection (Supporting Information Figs S3 and S4). An unbiased analysis of gene changes in Q111 cells subjected to structurally diverse TG2 inhibitors resulted in broad normalization of not only cytochrome *c* and PGC-1α, but also several hundred other genes dysregulated by mhtt in Q111 cells (Fig 6A, microarray analysis – GEO Dataset GSE21237). The findings support conclusions by others that HD reflects gene dysregulation of many functions (not only the mitochondria) (Benn et al, 2008). Indeed, the classes of compounds most effective to date in pre-clinical models are those that directly reduce mhtt levels (Krainc, 2010) or modulate mhtt transcriptional dysregulation. Even the FDA approved, use dependent, NMDA antagonist, memantine appears to prevent transcriptional dysregulation of PGC-1α (and likely other CREB dependent genes) induced by extrasynaptic glutamate and excacerbated by mhtt (Milnerwood et al, 2010; Okamoto et al, 2009).

Non-selective class I or II HDAC inhibitors (phenylbutyrate, valproic acid and HDAC inhibitor 4b) are being tested in humans for HD and other neurological conditions (Kazantsev & Thompson, 2008). Is TG2 inhibition in any way superior to HDAC inhibition, if both act on histones to promote transcription? Recent studies have highlighted some shortcomings of non-selective HDAC inhibition: HDAC1 inhibition leads to DNA damage in the CNS (Kim et al, 2008); the ability of HSP40 chaperones to reduce toxicity of polyQ proteins in cultured cells is reduced by HDAC4 inhibition (Hageman et al, 2010). Together these studies suggest that non-selective HDAC inhibition has biological actions that potentially create toxicity and limit efficacy of this approach. A number of groups are actively developing isoform-selective HDAC inhibitors (that would avoid inhibiting HDAC1 or HDAC4) for treatment of HD (Rivieccio et al, 2009). Fortuitously, TG2 inhibition represents an HDAC-independent, epigenetic strategy that normalizes gene expression and like isoforms-selective HDAC inhibitors, would similarly avoid the deleterious consequences of HDAC1 or HDAC4 inhibition. Additionally, the magnitude of transcriptional normalization by TG2 inhibition (nearly 40%) appears to be equivalent to that of HDAC inhibition (Thomas et al, 2008). Given the existence of established inhibitors for HDACs and the elucidation of a selective TG2 inhibitor herein (ZDON), a head-to-head comparison of TSA or butyrate to ZDON, or a combination of two of these is in order. Indeed, a prior study showed a 40% increase in survival in R6/2 mice treated with a combination of a DNA binding drug, mithramycin and the non-selective TG2 inhibitor, cystamine (Ryu et al, 2006).

Another exciting aspect of the current study is their ability to clarify and extend prior observations from several groups working on TG2 and HD. Karpuj and Steinman first showed that the non-selective TG2 inhibitor, cystamine reverses transcriptional dysregulation in an HD model. Specifically, they showed that one of the HSP40 chaperones, DNAJB10 (which by itself can reduce poly Q toxicity) was increased in cystamine treated mice (Karpuj et al, 2002); however they did not provide a model for how TG2 inhibition could increase DNAJB10 transcription. DNAJ message and protein levels were subsequently confirmed to be reduced in brains from HD patients. The FDA approved, TG2 inhibitor cysteamine also increased DNAJ (HSJ1b) transcription and protein levels in striatal neurons *in vitro* and protected worms (*Caenorhabditis elegans*) from the toxic effects of mhtt (Borrell-Pages et al, 2006). Cysteamine enhanced trafficking of BDNF by inhibiting TG2 function at the Golgi apparatus, but the role of TG2 in DNAJ transcription was, again not examined. Microarray studies herein showed that ZDON can significantly increase DNAJB10 expression, a finding that was validated by quantitative real time RT-PCR (Supporting Information Fig S11). These studies as well as our results showing that TG2 binds to chromatin to repress transcription support a role for this enzyme in silencing the expression of an important chaperone (HSJ1b) that increases mhtt proteotoxicity. While the relationship between ZDON-induced increased PGC-1α expression and ZDON-induced protection remains unclear, the mechanism by which ZDON-induced changes in DNAJ (HSJ1b) expression would lead to neuroprotection are well established by these prior studies (Borrell-Pages et al, 2006; Hageman et al; Karpuj et al, 2002). Moreover, prior studies showed that increases in cytosolic calcium consequent to glutamate receptor hyperactivation lead to activation of TG2 and cell death (Milnerwood et al, 2010; Okamoto et al, 2009). Consistent with these observations, TG2 inhibition protected striatal neurons from WT and YAC128 mice from NMDA toxicity by TG2 inhibition (Fig 8). From these data, a model can be generated whereby TG2 participates with mhtt to silence the expression of many genes in neurons (and presumably astrocytes) including those involved in the generation of ATP and those involved in glial glutamate transport. Reductions in ATP contribute to excessive NMDA receptor activation (particularly extrasynaptically) by energy-dependent loss of the Mg^{++} block (Beal et al, 1993) or by diminished scavenging of glutamate by astrocytes (Bradford et al, 2009, 2010; Fig 8). Excessive activation of extrasynaptic NMDA receptors, leads to receptor mediated increases in cytosolic calcium and activation of TG2 (a calcium-regulated enzyme), further enhancing transcriptional repression of many genes, including PGC-1α, BDNF and DNAJ chaperones (Milnerwood et al, 2010; Okamoto et al, 2009; Figs 1A and 4A, Supporting Information Fig S11). Repression of these and other genes contributes to dysfunction and ultimately death of neurons. Inhibition of TG2 positively influences function and survival, not only by normalizing gene expression in neurons and possibly astrocytes (nuclear function of TG2), but also by enhancing trafficking of BDNF (via cytosolic

activities of TG2 and increased expression of DNAJ) (Conforti et al, 2008). Altogether these studies suggest that both nuclear and cytosolic TG2 contribute importantly to HD pathogenesis and should heighten interest in the development of novel small molecule inhibitors of TG2 to consolidate the advances subsequent to our identification and characterization of the selective TG2 inhibitor, ZDON.

MATERIALS AND METHODS

TG inhibitors

ZDON and Boc-DON were obtained from Zedira (Darmstadt, Germany). Cystamine was obtained by Sigma–Aldrich. The Boc-DON peptide was known from the literature (Parameswaran et al, 1990). IC50 studies involving recombinant TG2 were performed, as described in Supporting Information. Of note, our initial studies with ZDON defined incubation times appropriate to inhibit TG2 in a test tube assay (McConoughey et al, 2009). Our empirical experience has been that different cell types respond to ZDON differently likely because they express different levels of TG2 and have different capacity to transport and metabolize the peptide ZDON. For that reason we monitored incubations to find the shortest period of time before we observed an increase in cytochrome *c* and PGC-1α transcription by RT-PCR; this correlated well with global changes in TG2 activity (not shown). As expected, for the reasons outlined above these incubation times were different for different cell types.

Cell culture conditions

STHdh^{Q7} and *STHdh*^{Q111} cells were maintained in Dulbecco's modified Eagle medium (Invitrogen, Carlsbad, CA) containing 25 mM D-glucose, 1 mM L-glutamine and supplemented with 10% fetal bovine serum (FBS), 1 mM sodium pyruvate and 400 μg/ml geneticin (Invitrogen). All cells were incubated at 33°C with 5% CO_2. Cells were not used after they reached 15 passages. WT and TG2$^{-/-}$ MEFs were kept at 37°C with 5% CO_2 in Dulbecco's modified Eagle medium (DMEM) supplemented with 10% FBS.

Plasmids

Full-length cytochrome *c* promoter reporter plasmid (pGL3RC4/-326) was used as previously described (Herzig et al, 2000).

Doxycyline-Inducible Q103 (mutant Htt)-EGFP neuronal cell lines

The T-REx™ System (Invitrogen, Carlsbad, CA) was used to generate Q103-enhanced GFP (EGFP) cell lines. This system utilizes two vectors, the pcDNA6/TR vector, a regulatory plasmid that expresses the tetracycline repressor (TetR), and pcDNA4/TO, which contains a cytomegalovirus (CMV) promoter driving the expression of the gene of interest under the control of Tet-operator sequences. Q103-EGFP was subcloned into the pcDNA4/TO vector from pcDNA-Q25- and Q103-EGFP construct, in which exon 1 of mhtt is cloned to an EGFP fusion vector (Clontech, Mountain View, CA). pcDNA4/TO-Q103-EGFP was linearized and transfected into SH-SY5Y cell clone over expressing pcDNA6/TR. The Q103-EGFP cell clones were selected by zeocin. For the induction of Q25- and Q103-EGFP, 3–10 mM of doxycyline was treated into culture medium.

Transglutaminase 2 constructs

WT TG2 and the transamidating-defective isoform (C277V TG2) have been previously described (Antonyak et al, 2002); NES TG2 was obtained by introducing the NES of HIV Rev (LPPLERLTL) (Fischer et al, 1995) to the N terminal of Myc-TG2. The NN TG2 has the NES sequence at the N-terminal of Myc-TG2 and a mutation at the NLS sequence in position 597–602 (PKQKRK → PKQAAK). The mutations were generated using a site-directed mutagenesis method (Quick-change Constructs mutation kit, Stratagene). Constructs were confirmed by DNA sequencing.

Total lysate

For total TG2 expression, cells were harvested in cold phosphate buffer saline (PBS), centrifuged at 3000 × *g* at 4°C and resuspended in lysis buffer (50 mM Tris–HCl pH 7.4, 1% Triton X-100, 100 mM NaCl and protease inhibitor cocktail).

Immunofluorescence

Q7 cells expressing the Myc-pCDNA3 vector, Myc-TG2 WT, Myc-TG2 NES or Myc-TG2 NN were fixed using 4% paraformaldehyde, permeabilized with 0.1% Triton X-100, and then incubated with a c-Myc antibody (Covance, USA). The c-Myc antibody was detected using an Alexa green 488-conjugated secondary antibody, and DAPI was used to stain the nuclei.

Immunoprecipitation

Myc-TG2 was immunoprecipitated from a total cell lysate (600 μg) using the IP/CoIP Myc kit, according to the manufacturer's instructions (Pierce).

Western blotting

Lysates from cells were centrifuged at 10,000 × *g* for 10 min at 4°C, and the protein concentration was measured using the Bradford Assay (Bio-Rad). Thirty micrograms of proteins was loaded into each well, run on NuPAGE® Bis-Tris Gels (4–12%), and transferred to a nitrocellulose filter for blotting. The primary antibodies used were anti-ND6 (Santa Cruz Biotechnology) at a 1:500 dilution in blocking buffer and anti-β-actin (Sigma) at 1:5000. All secondary antibodies were dye-labelled (LI-COR Biosciences, USA).

Histone precipitation

Harvested cells were resuspended in hypotonic lysis buffer. The lysate was centrifuged at 15,000 × g for 10 min at 4°C, and then resuspended in 200 ml of 0.4 N H_2SO_4 and rotated overnight at 4°C. The homogenate was then centrifuged at 21,000 × g for 10 min at 4°C, and the resulting supernatant was transferred to a fresh tube. The histones were precipitated, incubated on ice for 30 min, and then centrifuged at 13,000 rpm for 10 min at 4°C and the resulting pellet contained the histones. The histones were dissolved in Western blot loading buffer, and the acetylated histones were revealed with anti-acetyl H4 at 1:500 (Millipore) and total H4 were detected with anti-H4 at a 1:1000 dilution (Millipore).

Microarray analysis

Total RNA was extracted from Q111 and Q7 striatal cell lines, after 12 h treatment with ZDON (50 μM), Boc-DON (50 μM), cystamine (250 μM) or control treatment. Three replicates were run per sample

category, for a total of 24 arrays. RNA quantity was assessed with Nanodrop (Nanodrop Technologies) and quality with the Agilent Bioanalyzer (Agilent Technologies). Total RNA (200 ng) was amplified, biotinylated and hybridized on Illumina Mouse Mouseref-8 Expression Beadchips v1.1, querying the expression of ~22,000 Refseq transcripts, as per manufacturer's protocol. Slides were scanned using Illumina BeadStation and signal extracted using Illumina BeadStudio software (Illumina, San Diego, CA). Raw data were analysed using Bioconductor packages (www.bioconductor.org). Quality assessment was performed looking at the interarray Pearson correlation and clustering based on top variant genes was used to assess overall data coherence. One sample (Q7 cells treated with Boc-DON) failed the QC test and was excluded from further analysis. Contrast analysis of differential expression was performed using the LIMMA package (Smyth et al, 2005). After linear model fitting, a Bayesian estimate of differential expression was calculated. Data analysis was aimed at (1) identifying transcriptional changes in the Q111 compared to Q7 striatal cell line, and (2) the effect of drug treatment on gene expression abnormalities. The threshold for statistical significance was set at $p < 0.005$. The raw gene-expression data are available at www.ncbi.nlm.nih.gov/geo (GEO Dataset, GSE21237). GO and Pathway analysis were carried out using the Database for Annotation, Visualization and Integrated Discovery (DAVID) and Ingenuity Pathway Analysis (www.ingenuity.com). For Promoter analysis methods see Supporting Information Section.

Citrate synthase specific activity assay

Q7 and Q111 cells were harvested, and 50 μg of lysate was added to each well of a 96-well plate containing: 120 μl of 100 mM Tris Buffer (Sigma), 20 μl of 2 mM acetyl CoA (Sigma), and 20 μl of 2.5 mM 5,5′-dithio-bis-(2-nitrobenzoic acid) (DTNB) (Sigma). Background readings were done at 37°C for 5 min at 412 nm, after which 20 ml of 2 mM oxaloacetate (Sigma) was added to each well. OD was measured at 412 nm for 30 min. The rate of CS specific activity of ZDON treated cells was quantified relative to non-treated cells.

Mitotracker staining®

Q7 and Q111 were treated with ZDON 50 μM for 12 h, washed with pre-warmed Hank's buffered salt solution (HBSS) and incubated with MitoFluor Red 594 probe (Invitrogen) at a final concentration of 100 nM for 30 min. The dye was removed from the supernatant and the cells were analysed with the axiover 200 epi-fluorescence microscope (Zeiss).

Chromatin immunoprecipitation assay

A ChIP assay kit was used as directed by the manufacturer (Millipore). Briefly, cells were cross-linked with formaldehyde (1% for 10 min at 37°C). Cells were sonicated and immunoprecipitated with primary antibodies (15 μg) against TG2 (NeoMarkers) and anti-rabbit IgG (Santa Cruz or Millipore). The crosslinking was reversed, and the DNA was isolated either through phenol/chloroform extraction or on DNA columns (Millipore). Using an Applied Biosystems 7500 Fast Real Time PCR System, PCR reactions were conducted either using Taqman labelled primers targeted to the cytochrome *c* promoter (forward, GTTACCTGAGCCGAGCCACAC; reverse, TGACGTAACCGCACCTCATTGG) or using SYBR GREEN Master Mix and primers amplifying the PGC-1α gene (forward, TTGCTAGCGGTCCTCACAGA; reverse, GGCTCTTCTGCCTCCTGA).

Luciferase assay

Q7 and Q111 cells were transfected with the cytochrome *c* promoter–reporter and a pTK-Renilla control (Promega). Luciferase activity was measured by a dual luciferase assay (Promega) and normalized to Renilla activity using a bioluminator (Molecular Devices) according to the manufacturers' instructions.

Drosophila

Fly stocks were kept at 18°C and moved to 25°C for breeding and experimentation. After the Q93 flies (*w*; P{UAS-Httex1p Q93}4F1) were crossed with the *elav* (*w*; P{$w^{+mW.hs}$ = GawB}elavC155), the resulting offspring were moved to vials containing food supplemented with DMSO, 125 μM ZDON or water. At 10 days of age the flies were decapitated and the heads were mounted on a microscopic slide with nail polish. The rhabdomeres were analysed under oil emersion at 63X to visualize individual rhabdomeres. The scoring (counting the rhabdomeres for each ommatidium) was done blinded and the correct labels were given only after all of the data were acquired. There were 15–20 flies used for each condition with 800–1000 ommatidia counted for each group of flies (Control, DMSO and ZDON). RNA was isolated from the heads of *Drosophila* through Trizol lysis and phenol–chloroform extraction.

Transient transfection

Q7 and Q111 cells were plated in 96-well plates. Cells were transfected using Lipofectamine 2000 (Invitrogen) as directed by the manufacturer.

Cell viability

Q7, Q111 or primary neurons were plated in a 96-well Blackwell plate and treated with 50 μM ZDON. After 12 h, the medium was replaced with low glucose media containing 10 mM 3-NP. After 48 h, live cells were visualized with LIVE/DEAD assay (Invitrogen). The wells were then photographed using a flash cytometer and live cells were counted with Trophos software (France).

Quantitative real time PCR

Either the Taqman RNA-to-Ct, one-step kit (Applied Biosystems) was used according to the manufacturer's instructions or reverse transcription using Superscript 3 (Invitrogen) was conducted on 2 μg of total RNA extracted from Q7 and Q111 cells. The cDNA was then run with the Taqman® Gene Expression Master Mix and Taqman® Gene Expression Assays for cytochrome *c*, PGC-1α, HSJ1b, 18S, on an Applied Biosystems 7500 Fast Real Time PCR System. The resulting data were analysed using the delta delta CT method, and all measurements were normalized to 18S mRNA.

RNAi

Three sequences of Stealth RNAi (Invitrogen; RNAi1: GGAGGGAGACCUGAGUACCAAGUAU; RNAi2: CCUGCCUGAUGCUCUUGGAUAUGAA; RNAi3: CCUGCCUGAUGCUCUUGGAUAUGAA) targeted against TG2 were transfected into Q111 cells using Lipofectamine 2000 (Invitrogen). Cells were grown in culture 24–48 h after transfection, and RNA was isolated to measure levels of cytochrome *c*, PGC-1α, TG2 or 18S by qRT-PCR.

Myoblast cell culture

Myoblasts derived from muscle biopsies were obtained from control subjects and HD patients (Ciammola et al, 2006). The myoblasts were cultured as previously described (Blau & Webster, 1981). Briefly, myoblasts were grown in HAMs F10 medium (GIBCO, Invitrogen) supplemented with 15% FBS (Invitrogen, San Diego, CA), 0.5 mg/ml bovine serum albumin, 4 ng/ml insulin, 10 ng/ml epidermal growth factor, 0.39 mg/ml dexamethasone, 0.1 mg/ml streptomycin and 100 U/ml penicillin.

NMDA induced cytotoxicity

Cultured MSNs (DIV 7 or 8) were pre-treated with 25 μM, 50 μM ZDON or 50 μM control Zc peptides for 12 h, then incubated in warm balanced salt solution (BSS, pH 7.4) with or without 500 μM NMDA for 10 min. MSNs were washed twice with warm plating medium (PM) and then incubated in conditioned PM for 24 h.

TUNEL assay and assessment of apoptosis

Fixed MSNs were numbered according to different conditions and coded before staining to ensure that the operator was blinded during the subsequent processing and analysis of immunofluorescence. MSNs were further permeabilized with 0.25% Triton X-100 in PBS with 0.5% sodium citrate on ice for 2 min. MSNs were then washed once with PBS and incubated in PBS with 16 μg/ml RNAse at RT for 30 min. MSNs were washed with PBS and incubated in TUNEL (Roche) reagent (at a ratio of label/enzyme = 9:1) per well in the dark for 1 h, followed by one wash with PBS and staining with 10 μM Hoechst 33342. MSNs were then washed with PBS and mounted on slides with Fluoromount-G. The second day after staining, the percentage of apoptotic cell death was assessed by counting the numbers of TUNEL positive cells in the green fluorescent channel which also showed condensed and blebbed nuclear morphology in the blue fluorescent channel, then dividing by the total number of Hoechst positive cell nuclei in the blue fluorescent channel and multiplying by 100. A total of 1000 neurons were counted per condition. In each experiment, apoptosis 24 h following 10-min treatment with BSS alone, without NMDA, was assessed and the percentage was subtracted as a baseline from the total cell death induced by NMDA in each experiment to calculate the specific NMDAR-mediated apoptosis.

Statistics

All data were expressed as mean ± SEM and were plotted using GraphPad Prism software. Analysis of variance was used to compare means with one or two-way analysis of variance (ANOVA) and Tukey's or Bonferroni's *post hoc* tests were applied accordingly when significance was found. All results are from experiments conducted a minimum of three times, and all graphs show Mean ± SEM.

Author contributions

Study conception, study design, statistical analyses: S.J.M., M.B., R.R.R. Acquisition of data: S.J.M., M.B., Z.V.N., S.F.S., N.A.S., B.C.L., M.A.A., B.L., A.S., R.C., G.C., X.L., J.F. Analyses and interpretation of data: S.J.M., M.B., Z.V.N., S.F.S., B.C.L., M.A.A., B.L., M.F.B., G.C., A.S., J.F, L.A.R, L.J.M., L.M.T. Contributed reagents/materials/analysis tools: L.M., A.J.L.C., M.A.A., R.A.C., F.M.B., D.H.G., H.R., S.E.L., J.P., R.P., M.H., L.A.R., L.J.M., L.M.T., R.R.R. Manuscript preparation: S.J.M., M.B., S.F.S., B.C.L., L.J.M., L.M.T., R.R.R. Manuscript editing: M.B., R.R.R.

Acknowledgements

This work was supported by funding from the Sheldon and Miriam Adelson Medical Research Foundation (to R.R.R, G.C., B.L. and D.G.), the Hereditary Disease Foundation [HDF-24085], the Huntington's Disease Society of America and the HighQ Foundation and the Cure Huntington Disease Initiative (CHDI, to L.A.R.); grants from the National Institutes of Health (P01 NIA AG014930, Project 1 to R.R.R., Project 3 to A.S. and Project 4 to M.F.B.) and awards (NS045283 to J.L.M., NS52789 to L.M.T.). We thank Vicky Brandt for her thoughtful editorial contributions and Richard Scarpulla for helpful comments and suggestions throughout the assembly of this manuscript. We thank Dr. Marcy MacDonald for providing the Q7 and Q111 cells and Irina Gazaryan for discussions on the chemistry of ZDON and TG2 catalytic site.

Supporting information is available at EMBO Molecular Medicine online.

Conflict of Interest Disclosure: Ralf Pasternack and Martin Hils are employed by Zedira, a German biotechnology company, which sells the peptides ZDON or Boc-DON as inhibitors of transglutaminase for preclinical use. None of the other authors of this manuscript have any conflicts of interest; specifically, none of the other authors has or are entitled to any royalties, grant support or financial compensation from Zedira. Moreover, outside of providing reagents, Zedira has not influenced the content or conclusions of the study.

For more information

Accompanying Closeup:
http://dx.doi.org/10.1002/emmm.201000092

OMIM, Online Mendelian Inheritance in Man
Transglutaminase 2; TGM2
http://www.ncbi.nlm.nih.gov/omim/190196

HUNTINGTON DISEASE; HD
http://www.ncbi.nlm.nih.gov/omim/143100

Rajiv R. Ratan's webpage:
http://www.burke.org/page.cfm?p=320

References

Agrawal N, Pallos J, Slepko N, Apostol BL, Bodai L, Chang LW, Chiang AS, Thompson LM, Marsh JL (2005) Identification of combinatorial drug regimens for treatment of Huntington's disease using *Drosophila*. Proc Natl Acad Sci USA 102: 3777-3781

Antonyak MA, Boehm JE, Cerione RA (2002) Phosphoinositide 3-kinase activity is required for retinoic acid-induced expression and activation of the tissue transglutaminase. J Biol Chem 277: 14712-14716

Bailey CD, Johnson GV (2006) The protective effects of cystamine in the R6/2 Huntington's disease mouse involve mechanisms other than the inhibition of tissue transglutaminase. Neurobiol Aging 27: 871-879

Ballestar E, Franco L (1997) Use of the transglutaminase reaction to study the dissociation of histone N-terminal tails from DNA in nucleosome core particles. Biochemistry 36: 5963-5969

Ballestar E, Abad C, Franco L (1996) Core histones are glutaminyl substrates for tissue transglutaminase. J Biol Chem 271: 18817-18824

Ballestar E, Boix-Chornet M, Franco L (2001) Conformational changes in the nucleosome followed by the selective accessibility of histone glutamines in the transglutaminase reaction: effects of ionic strength. Biochemistry 40: 1922-1929

Battaglia G, Farrace MG, Mastroberardino PG, Viti I, Fimia GM, Van Beeumen J, Devreese B, Melino G, Molinaro G, Busceti CL *et al* (2007) Transglutaminase 2 ablation leads to defective function of mitochondrial respiratory complex I affecting neuronal vulnerability in experimental models of extrapyramidal disorders. J Neurochem 100: 36-49

Beal MF, Brouillet E, Jenkins BG, Ferrante RJ, Kowall NW, Miller JM, Storey E, Srivastava R, Rosen BR, Hyman BT (1993) Neurochemical and histologic characterization of striatal excitotoxic lesions produced by the mitochondrial toxin 3-nitropropionic acid. J Neurosci 13: 4181-4192

Benn CL, Sun T, Sadri-Vakili G, McFarland KN, DiRocco DP, Yohrling GJ, Clark TW, Bouzou B, Cha JH (2008) Huntingtin modulates transcription, occupies gene promoters *in vivo*, and binds directly to DNA in a polyglutamine-dependent manner. J Neurosci 28: 10720-10733

Blau HM, Webster C (1981) Isolation and characterization of human muscle cells. Proc Natl Acad Sci USA 78: 5623-5627

Borrell-Pages M, Canals JM, Cordelieres FP, Parker JA, Pineda JR, Grange G, Bryson EA, Guillermier M, Hirsch E, Hantraye P *et al* (2006) Cystamine and cysteamine increase brain levels of BDNF in Huntington disease via HSJ1b and transglutaminase. J Clin Invest 116: 1410-1424

Bradford J, Shin JY, Roberts M, Wang CE, Li XJ, Li S (2009) Expression of mutant huntingtin in mouse brain astrocytes causes age-dependent neurological symptoms. Proc Natl Acad Sci USA 106: 22480-22485

Bradford J, Shin JY, Roberts M, Wang CE, Sheng G, Li S, Li XJ (2010) Mutant huntingtin in glial cells exacerbates neurological symptoms of Huntington disease mice. J Biol Chem 285: 10653-10661

Brennan WA, Jr., Bird ED, Aprille JR (1985) Regional mitochondrial respiratory activity in Huntington's disease brain. J Neurochem 44: 1948-1950

Browne SE (2008) Mitochondria and Huntington's disease pathogenesis: insight from genetic and chemical models. Ann N Y Acad Sci 1147: 358-382

Browne SE, Beal MF (2006) Oxidative damage in Huntington's disease pathogenesis. Antioxid Redox Signal 8: 2061-2073

Browne SE, Bowling AC, MacGarvey U, Baik MJ, Berger SC, Muqit MM, Bird ED, Beal MF (1997) Oxidative damage and metabolic dysfunction in Huntington's disease: selective vulnerability of the basal ganglia. Ann Neurol 41: 646-653

Cattaneo E, Conti L (1998) Generation and characterization of embryonic striatal conditionally immortalized ST14A cells. J Neurosci Res 53: 223-234

Chaturvedi RK, Adhihetty P, Shukla S, Hennessy T, Calingasan N, Yang L, Starkov A, Kiaei M, Cannella M, Sassone J *et al* (2009) Impaired PGC-1alpha function in muscle in Huntington's disease. Hum Mol Genet 18: 3048-3065

Chavez AO, Kamath S, Jani R, Sharma LK, Monroy A, Abdul-Ghani MA, Centonze VE, Sathyanarayana P, Coletta DK, Jenkinson CP *et al* (2010) Effect of short-term free fatty acids elevation on mitochondrial function in skeletal muscle of healthy individuals. J Clin Endocrinol Metab 95: 422-429

Chen-Plotkin AS, Sadri-Vakili G, Yohrling GJ, Braveman MW, Benn CL, Glajch KE, DiRocco DP, Farrell LA, Krainc D, Gines S *et al* (2006) Decreased association of the transcription factor Sp1 with genes downregulated in Huntington's disease. Neurobiol Disease 22: 233-241

Chomyn A (2001) Mitochondrial genetic control of assembly and function of complex I in mammalian cells. J Bioenerg Biomembr 33: 251-257

Chomyn A, Mariottini P, Cleeter MW, Ragan CI, Matsuno-Yagi A, Hatefi Y, Doolittle RF, Attardi G (1985) Six unidentified reading frames of human mitochondrial DNA encode components of the respiratory-chain NADH dehydrogenase. Nature 314: 592-597

Chomyn A, Cleeter MW, Ragan CI, Riley M, Doolittle RF, Attardi G (1986) URF6, last unidentified reading frame of human mtDNA, codes for an NADH dehydrogenase subunit. Science (New York, NY) 234: 614-618

Ciammola A, Sassone J, Alberti L, Meola G, Mancinelli E, Russo MA, Squitieri F, Silani V (2006) Increased apoptosis, Huntingtin inclusions and altered differentiation in muscle cell cultures from Huntington's disease subjects. Cell Death Differ 13: 2068-2078

Conforti P, Ramos C, Apostol BL, Simmons DA, Nguyen HP, Riess O, Thompson LM, Zuccato C, Cattaneo E (2008) Blood level of brain-derived neurotrophic factor mRNA is progressively reduced in rodent models of Huntington's disease: restoration by the neuroprotective compound CEP-1347. Mol Cell Neurosci 39: 1-7

Cui L, Jeong H, Borovecki F, Parkhurst CN, Tanese N, Krainc D (2006) Transcriptional repression of PGC-1alpha by mutant huntingtin leads to mitochondrial dysfunction and neurodegeneration. Cell 127: 59-69

Dedeoglu A, Kubilus JK, Jeitner TM, Matson SA, Bogdanov M, Kowall NW, Matson / SNM› WR, Cooper AJ, Ratan RR, Beal MF *et al* (2002) Therapeutic effects of cystamine in a murine model of Huntington's disease. J Neurosci 22: 8942-8950

Dunah AW, Jeong H, Griffin A, Kim YM, Standaert DG, Hersch SM, Mouradian MM, Young AB, Tanese N, Krainc D (2002) Sp1 and TAFII130 transcriptional activity disrupted in early Huntington's disease. Science (New York, NY) 296(5576), 2238-2243

Fernandes D, Zaidi A, Bean J, Hui D, Michaelis ML (2007) RNA-induced silencing of the plasma membrane Ca2+-ATPase 2 in neuronal cells: effects on Ca2+ homeostasis and cell viability. J Neurochem 102: 454-465

Fischer U, Huber J, Boelens WC, Mattaj IW, Luhrmann R (1995) The HIV-1 Rev activation domain is a nuclear export signal that accesses an export pathway used by specific cellular RNAs. Cell 82: 475-483

Folk JE, Finlayson JS (1977) The epsilon-(gamma-glutamyl)lysine crosslink and the catalytic role of transglutaminases. Adv Protein Chem 31: 1-133

Fox JH, Barber DS, Singh B, Zucker B, Swindell MK, Norflus F, Buzescu R, Chopra R, Ferrante RJ, Kazantsev A *et al* (2004) Cystamine increases L-cysteine levels in Huntington's disease transgenic mouse brain and in a PC12 model of polyglutamine aggregation. J Neurochem 91: 413-422

Graham RK, Deng Y, Slow EJ, Haigh B, Bissada N, Lu G, Pearson J, Shehadeh J, Bertram L, Murphy Z *et al* (2006) Cleavage at the caspase-6 site is required for neuronal dysfunction and degeneration due to mutant huntingtin. Cell 125: 1179-1191

Hageman J, Rujano MA, van Waarde MA, Kakkar V, Dirks RP, Govorukhina N, Oosterveld-Hut HM, Lubsen NH, Kampinga HH (2010) A DNAJB chaperone subfamily with HDAC-dependent activities suppresses toxic protein aggregation. Mol Cell 37: 355-369

Heng MY, Detloff PJ, Wang PL, Tsien JZ, Albin RL (2009) *In vivo* evidence for NMDA receptor-mediated excitotoxicity in a murine genetic model of Huntington disease. J Neurosci 29: 3200-3205

Herzig RP, Scacco S, Scarpulla RC (2000) Sequential serum-dependent activation of CREB and NRF-1 leads to enhanced mitochondrial respiration through the induction of cytochrome *c*. J Biol Chem 275: 13134-13141

Ikle J, Elwell JA, Bryantsev AL, Cripps RM (2008) Cardiac expression of the *Drosophila* transglutaminase (CG7356) gene is directly controlled by myocyte enhancer factor-2. Dev Dyn 237: 2090-2099

Jeitner TM, Delikatny EJ, Ahlqvist J, Capper H, Cooper AJ (2005) Mechanism for the inhibition of transglutaminase 2 by cystamine. Biochem Pharmacol 69: 961-970

Jeitner TM, Matson WR, Folk JE, Blass JP, Cooper AJ (2008) Increased levels of gamma-glutamylamines in Huntington disease CSF. J Neurochem 106: 37-44

Jenkins BG, Koroshetz WJ, Beal MF, Rosen BR (1993) Evidence for impairment of energy metabolism *in vivo* in Huntington's disease using localized 1H NMR spectroscopy. Neurology 43: 2689-2695

Karpuj MV, Garren H, Slunt H, Price DL, Gusella J, Becher MW, Steinman L (1999) Transglutaminase aggregates huntingtin into nonamyloidogenic polymers, and its enzymatic activity increases in Huntington's disease brain nuclei. Proc Natl Acad Sci USA 96: 7388-7393

Karpuj MV, Becher MW, Springer JE, Chabas D, Youssef S, Pedotti R, Mitchell D, Steinman L (2002) Prolonged survival and decreased abnormal movements in transgenic model of Huntington disease, with administration of the transglutaminase inhibitor cystamine. Nat Med 8: 143-149

Kazantsev AG, Thompson LM (2008) Therapeutic application of histone deacetylase inhibitors for central nervous system disorders. Nat Rev Drug Discov 7: 854-868

Kim D, Frank CL, Dobbin MM, Tsunemoto RK, Tu W, Peng PL, Guan JS, Lee BH, Moy LY, Giusti P *et al* (2008) Deregulation of HDAC1 by p25/Cdk5 in neurotoxicity. Neuron 60: 803-817

Krainc D 2010 Huntington's disease: tagged for clearance. Nat Med 16: 32-33

Lee J, Kim CH, Simon DK, Aminova LR, Andreyev AY, Kushnareva YE, Murphy AN, Lonze BE, Kim KS, Ginty DD *et al* (2005) Mitochondrial cyclic AMP response element-binding protein (CREB) mediates mitochondrial gene expression and neuronal survival. J Biol Chem 280: 40398-40401

Lee JM, Ivanova EV, Seong IS, Cashorali T, Kohane I, Gusella JF, MacDonald ME (2007) Unbiased gene expression analysis implicates the huntingtin polyglutamine tract in extra-mitochondrial energy metabolism. PLoS Genet 3: e135

Lesort M, Attanavanich K, Zhang J, Johnson GV (1998) Distinct nuclear localization and activity of tissue transglutaminase. J Biol Chem 273: 11991-11994

Lesort M, Tucholski J, Zhang J, Johnson GV (2000) Impaired mitochondrial function results in increased tissue transglutaminase activity *in situ*. J Neurochem 75: 1951-1961

Liang H, Ward WF (2006) PGC-1alpha: a key regulator of energy metabolism. Adv Physiol Educ 30: 145-151

Lin J, Wu PH, Tarr PT, Lindenberg KS, St-Pierre J, Zhang CY, Mootha VK, Jager S, Vianna CR, Reznick RM *et al* (2004) Defects in adaptive energy metabolism with CNS-linked hyperactivity in PGC-1alpha null mice. Cell 119: 121-135

Lorand L, Conrad SM (1984) Transglutaminases. Mol Cell Biochem 58: 9-35

Mao Z, Choo YS, Lesort M (2006) Cystamine and cysteamine prevent 3-NP-induced mitochondrial depolarization of Huntington's disease knock-in striatal cells. Eur J Neurosci 23: 1701-1710

Marsh JL, Thompson LM (2006) *Drosophila* in the study of neurodegenerative disease. Neuron 52: 169-178

Mastroberardino PG, Iannicola C, Nardacci R, Bernassola F, De Laurenzi V, Melino G, Moreno S, Pavone F, Oliverio S, Fesus L *et al* (2002) 'Tissue' transglutaminase ablation reduces neuronal death and prolongs survival in a mouse model of Huntington's disease. Cell Death Differ 9: 873-880

McConoughey SJ, Niatsetskaya ZV, Pasternack R, Hils M, Ratan RR, Cooper AJ (2009) A nonradioactive dot blot assay for transglutaminase activity. Anal Biochem 390: 91-93

Milnerwood AJ, Gladding CM, Pouladi MA, Kaufman AM, Hines RM, Boyd JD, Ko RW, Vasuta OC, Graham RK, Hayden MR *et al* 2010 Early increase in extrasynaptic NMDA receptor signaling and expression contributes to phenotype onset in Huntington's disease mice. Neuron 65: 178-190

Niatsetskaya Z, Basso M, Speer RE, McConoughey SJ, Coppola G, Ma TC, Ratan RR 2010 HIF prolyl hydroxylase inhibitors prevent neuronal death induced by mitochondrial toxins: therapeutic implications for Huntington's disease and Alzheimer's disease. Antioxid Redox Signal 12: 435-443

Okamoto S, Pouladi MA, Talantova M, Yao D, Xia P, Ehrnhoefer DE, Zaidi R, Clemente A, Kaul M, Graham RK *et al* (2009) Balance between synaptic versus extrasynaptic NMDA receptor activity influences inclusions and neurotoxicity of mutant huntingtin. Nat Med 15: 1407-1413

Parameswaran KN, Velasco PT, Wilson J, Lorand L (1990) Labeling of epsilon-lysine crosslinking sites in proteins with peptide substrates of factor XIIIa and transglutaminase. Proc Natl Acad Sci USA 87: 8472-8475

Parker AJ, Arango M, Abderrahmane S, Lambert E, Tourette C, Catoire H, Neri C (2005) Resveratrol rescues mutant polyglutamine cytotoxicity in nematode and mammalian neurons. Med Sci (Paris) 21: 556-557

Peng X, Zhang Y, Zhang H, Graner S, Williams JF, Levitt ML, Lokshin A (1999) Interaction of tissue transglutaminase with nuclear transport protein importin-alpha3. FEBS Lett 446: 35-39

Petersen A, Bjorkqvist M (2006) Hypothalamic-endocrine aspects in Huntington's disease. Eur J Neurosci 24: 961-967

Puigserver P, Spiegelman BM (2003) Peroxisome proliferator-activated receptor-gamma coactivator 1 alpha (PGC-1 alpha): transcriptional coactivator and metabolic regulator. Endocr Rev 24: 78-90

Ratan RR (2009) Epigenetics and the nervous system: epiphenomenon or missing piece of the neurotherapeutic puzzle? Lancet Neurol 8: 975-977

Rivieccio MA, Brochier C, Willis DE, Walker BA, D'Annibale MA, McLaughlin K, Siddiq A, Kozikowski AP, Jaffrey SR, Twiss JL *et al* (2009) HDAC6 is a target for protection and regeneration following injury in the nervous system. Proc Natl Acad Sci USA 106: 19599-19604

Ruan Q, Lesort M, MacDonald ME, Johnson GV (2004) Striatal cells from mutant huntingtin knock-in mice are selectively vulnerable to mitochondrial complex II inhibitor-induced cell death through a non-apoptotic pathway. Hum Mol Genet 13: 669-681

Ryu H, Lee J, Olofsson BA, Mwidau A, Dedeoglu A, Escudero M, Flemington E, Azizkhan-Clifford J, Ferrante RJ, Ratan RR (2003) Histone deacetylase inhibitors prevent oxidative neuronal death independent of expanded polyglutamine repeats via an Sp1-dependent pathway. Proc Natl Acad Sci USA 100: 4281-4286

Ryu H, Lee J, Hagerty SW, Soh BY, McAlpin SE, Cormier KA, Smith KM, Ferrante RJ (2006) ESET/SETDB1 gene expression and histone H3 (K9) trimethylation in Huntington's disease. Proc Natl Acad Sci USA 103: 19176-19181

Seong IS, Ivanova E, Lee JM, Choo YS, Fossale E, Anderson M, Gusella JF, Laramie JM, Myers RH, Lesort M *et al* (2005) HD CAG repeat implicates a dominant property of huntingtin in mitochondrial energy metabolism. Hum Mol Genet 14: 2871-2880

Sleiman SF, Basso M, Mahishi L, Kozikowski AP, Donohoe ME, Langley B, Ratan RR (2009) Putting the 'HAT' back on survival signalling: the promises and challenges of HDAC inhibition in the treatment of neurological conditions. Expert Opin Investig Drugs 18: 573-584

Smyth GK, Michaud J, Scott HS (2005) Use of within-array replicate spots for assessing differential expression in microarray experiments. Bioinformatics 21: 2067-2075

Spiegelman BM (2007) Transcriptional control of mitochondrial energy metabolism through the PGC1 coactivators. Novartis Found Symp 287: 60-63, discussion 63–69

Steffan JS, Kazantsev A, Spasic-Boskovic O, Greenwald M, Zhu YZ, Gohler H, Wanker EE, Bates GP, Housman DE, Thompson LM (2000) The Huntington's disease protein interacts with p53 and CREB-binding protein and represses transcription. Proc Natl Acad Sci USA 97: 6763-6768

Steffan JS, Bodai L, Pallos J, Poelman M, McCampbell A, Apostol BL, Kazantsev A, Schmidt E, Zhu YZ, Greenwald M *et al* (2001) Histone deacetylase inhibitors arrest polyglutamine-dependent neurodegeneration in *Drosophila*. Nature 413: 739-743

St-Pierre J, Drori S, Uldry M, Silvaggi JM, Rhee J, Jager S, Handschin C, Zheng K, Lin J, Yang W *et al* (2006) Suppression of reactive oxygen species and neurodegeneration by the PGC-1 transcriptional coactivators. Cell 127: 397-408

Tabrizi SJ, Cleeter MW, Xuereb J, Taanman JW, Cooper JM, Schapira AH (1999) Biochemical abnormalities and excitotoxicity in Huntington's disease brain. Ann Neurol 45: 25-32

Tatsukawa H, Fukaya Y, Frampton G, Martinez-Fuentes A, Suzuki K, Kuo TF, Nagatsuma K, Shimokado K, Okuno M, Wu J *et al* (2009) Role of transglutaminase 2 in liver injury via cross-linking and silencing of transcription factor Sp1. Gastroenterology 136: 1783-1795, e1710

Thomas EA, Coppola G, Desplats PA, Tang B, Soragni E, Burnett R, Gao F, Fitzgerald KM, Borok JF, Herman D *et al* (2008) The HDAC inhibitor 4b ameliorates the disease phenotype and transcriptional abnormalities in Huntington's disease transgenic mice. Proc Natl Acad Sci USA 105: 15564-15569

Trettel F, Rigamonti D, Hilditch-Maguire P, Wheeler VC, Sharp AH, Persichetti F, Cattaneo E, MacDonald ME (2000) Dominant phenotypes produced by the HD mutation in STHdh(Q111) striatal cells. Hum Mol Genet 9: 2799-2809

Van Raamsdonk JM, Pearson J, Bailey CD, Rogers DA, Johnson GV, Hayden MR, Leavitt BR (2005) Cystamine treatment is neuroprotective in the YAC128 mouse model of Huntington disease. J Neurochem 95: 210-220

van Roon-Mom WM, Reid SJ, Jones AL, MacDonald ME, Faull RL, Snell RG (2002) Insoluble TATA-binding protein accumulation in Huntington's disease cortex. Brain Res 109: 1-10

Vonsattel JP, DiFiglia M (1998) Huntington disease. J Neuropathol Exp Neurol 57: 369-384

Zainelli GM, Dudek NL, Ross CA, Kim SY, Muma NA (2005) Mutant huntingtin protein: a substrate for transglutaminase 1, 2, and 3. J Neuropathol Exp Neurol 64: 58-65

Zeron MM, Hansson O, Chen N, Wellington CL, Leavitt BR, Brundin P, Hayden MR, Raymond LA (2002) Increased sensitivity to *N*-methyl-D-aspartate receptor-mediated excitotoxicity in a mouse model of Huntington's disease. Neuron 33: 849-860

Zuccato C, Cattaneo E (2009) Brain-derived neurotrophic factor in neurodegenerative diseases. Nat Rev Neurol 5: 311-322

